A UNILATERAL TUNNEL-DIODE FREQUENCY CONVERTER

by

WARREN DAVID LITTLE

B.A.Sc., The University of British Columbia, 1961

A THESIS SUBMITTED IN PARTIAL FULFILMENT OF
THE REQUIREMENTS FOR THE DEGREE OF
MASTER OF APPLIED SCIENCE

in the Department of
Electrical Engineering

We accept this thesis as conforming to the
required standard

THE UNIVERSITY OF BRITISH COLUMBIA

June, 1963

In presenting this thesis in partial fulfilment of the requirements for an advanced degree at the University of British Columbia, I agree that the Library shall make it freely available for reference and study. I further agree that permission for extensive copying of this thesis for scholarly purposes may be granted by the Head of my Department or by his representatives. It is understood that copying or publication of this thesis for financial gain shall not be allowed without my written permission.

Department of Electrical Engineering

The University of British Columbia,
Vancouver 8, Canada.

Date July 25, 1963

ABSTRACT

Frequency converters using pumped nonlinear conductance and pumped nonlinear capacitance with the property of signal flow in one direction only are the subject of this thesis. The unilateral property can be obtained either by a suitable termination at the image frequency or by quadrature pumping the conductance and capacitance.

Of great importance is a frequency converter in which the output frequency is lower than that of the input. Such a down-converter based upon a proposed image termination method is examined both analytically and experimentally. Conditions are given which the conductance and capacitance must satisfy in order that the image termination be passive. The conditions are fulfilled by a single tunnel-diode. It is found that a forward- to reverse-gain ratio of at least 20 db over a 5% bandwidth is feasible: the estimated noise figure is 3.4 db.

The quadrature pumped converter is compared with the image terminated converter and it is shown in particular that the former can be unilateral only at one frequency.

ACKNOWLEDGEMENT

The author wishes to thank the supervising professor, Dr. M. P. Beddoes, for his help and encouragement during the course of this study.

Grateful acknowledgement is given to the British Columbia Telephone Company for a scholarship awarded in 1961, and to the National Research Council for a Studentship in 1962.

The work described in this thesis was supported by the National Research Council under Grant BT-68.

TABLE OF CONTENTS

Page

LIST OF ILLUSTRATIONS

List of Symbols

Symbol	Description	First defined in Section
$V_g(t)$	total voltage across nonlinear conductance	2.1
$V_{gp}(t)$	conductance pump voltage	2.1
$v(t)$	small-signal voltage	2.1
$I_g(t)$	total current through nonlinear conductance	2.1
$g(t)$	instantaneous incremental conductance	2.1
$I_{gp}(t)$	conductance pump current	2.1
$i_g(t)$	small-signal conductance current	2.1
$I_{cp}(t)$	capacitance pump current	2.1
q	charge on nonlinear capacitance	2.1
$V_{cp}(t)$	capacitance pump voltage	2.1
V_{cb}	capacitance bias voltage	2.1
V_{gb}	conductance bias voltage	2.1
$i_c(t)$	small-signal capacitance current	2.1
$C(t)$	instantaneous incremental capacitance	2.1
g_n	n^{th} conductance harmonic (real)	2.2
C_n'	n^{th} capacitance harmonic (complex)	2.2
C_n	n^{th} capacitance harmonic (real)	2.2
V_i	i^{th} voltage harmonic (small-signal)	2.2
I_i	i^{th} current harmonic (small-signal)	2.2
ω_0	pump angular frequency	2.2
ω_1	r.f. angular frequency	2.2
ω_2	i.f. angular frequency	2.2
ω_3	image angular frequency	2.2
Y_i	admittance across mixing-element at frequency ω_i	3.1

List of Symbols

Symbol	Definition	First defined in Section
$\overline{Y}_i$	Y_i minus admittance of filters	3.1
Y_{ij}	admittance parameters of the mixing-element matrix	3.1
G_{T12}	forward transducer gain	3.2
G_{T21}	reverse transducer gain	3.2
α	nonlinear factor	4.1
β	loading factor	4.1
Ω_i	normalized frequency	4.1
Y_{in}	converter input admittance	4.2
Y_{out}	converter output admittance	4.2
F	converter noise figure	5

A UNILATERAL TUNNEL-DIODE FREQUENCY CONVERTER

1. INTRODUCTION

Most modern high frequency communication receivers use the heterodyne principle,[1] in which power at the carrier frequency of the incoming signal gives rise to power at a lower intermediate frequency which is more suitable for amplification and detection. This frequency conversion is carried out in the down-converter stage of the receiver. The noise performance of the down-converter is of prime importance since it determines the ultimate sensitivity of the receiver.[2] Until the advent of the tunnel-diode in 1957,[3] crystal-diodes were used almost exclusively as the frequency changing elements.[4] The best crystal-diode converters have conversion losses of 3 to 4 decibels and noise figures of 4 to 5 decibels.[5] In 1960 Chang, et al[6] showed that tunnel-diode frequency converters with 22 decibels of conversion gain and noise figures of 3 decibels were possible. To the author's knowledge all tunnel-diode down-converters that have been studied are reciprocal.* This property is undesirable because the input is in no way isolated from the output and as a result the input noise is increased by noise in the output circuit.[2]

---

* For a reciprocal transducer the forward gain is equal to the reverse gain.

The main topic of this thesis is the development of a unilateral* tunnel-diode down-converter.

Previous studies of tunnel-diode converters have considered the nonlinear conductance of the diodes as the sole frequency converting element. In addition to a nonlinear conductance however, tunnel-diodes have a nonlinear junction capacitance:[3] and this, as will be shown, can play a very important part in the frequency converting process. For generality, equations are developed for a converter having separate nonlinear conductance and nonlinear capacitance elements. The equations are then applied to tunnel-diodes in which the two nonlinear elements are directly in parallel.

The concept of frequency conversion is introduced by considering the block diagram of Figure 1-1. The frequency converter, proper, consists of blocks 1, 2 and 3. The combination of blocks 1 and 2 is defined as the mixing-element. It is the active portion of the converter.

The input signal is a sinewave of frequency f_1 and the pump is another sinewave of frequency f_0. The nonlinearities cause voltage or current harmonics** to be developed at f_0 and f_1, and at sums and differences of the harmonic frequencies. The output frequency f_2 is one of these frequencies -- for example: $f_1 - f_0$. In general, the converter exhibits

---

* For a unilateral transducer the forward gain is finite and the reverse gain is zero.

** Corresponding to open-circuit terminations, voltage harmonics will be produced: short-circuit terminations will lead to current harmonics.

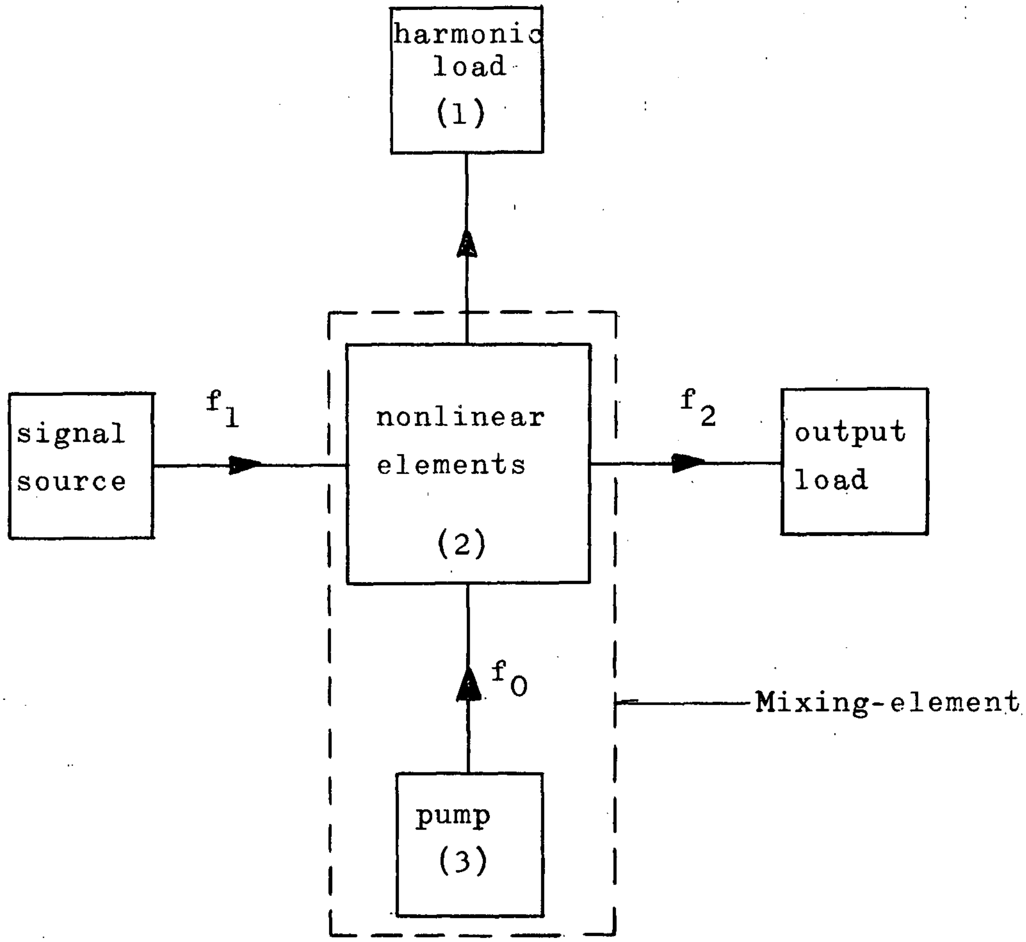

Figure 1-1. Block Diagram Illustrating Frequency Converting Process.

bilateral* but not reciprocal gain. In this thesis, it is shown that a special termination at one normally unused harmonic (image) produces zero gain in one direction.

The theory of unilateral frequency conversion, together with experimental techniques and findings, are discussed in the

---

* Gain is loosely bilateral. An input signal at f_1 produces an output response at f_2; and vice-versa an input signal at f_2 produces an output at f_1: the input and output signals are separated by frequency rather than distance but usage has it that the gain from f_1 to f_2 is described in terms of direction. The converter, having gain in both such directions, is thus bilateral.

chapters that follow. In Chapter 2 a mathematical description of the mixing-element is developed. This description is in the form of an admittance matrix relating small-signal voltage and current harmonics. It is derived, using Fourier Series methods, from the differential equation of the mixing-element.

In Chapter 3 it is shown that for the case under study the mixing-element is equivalent to a three-port network. The three-port is reduced to a two-port. Using the short-circuit admittance matrix of the reduced network, two methods by which the converter may be made unilateral are outlined.

A converter made unilateral by proper termination of an image circuit is studied in Chapter 4. This study is based upon the matrices established in Chapter 2 and Chapter 3 and includes important realizability, stability and gain conditions. It is found that with optimum terminations (Section 4.2) wide-band unilateral frequency conversion with gain can be obtained but that with simple terminations the unilateral property is realized only over a narrow frequency band.

Chapter 5 contains a very brief noise analysis of the converter.

In Chapter 6 an experimental converter is discussed. The results obtained with this converter, and problems associated with it, are presented and compared with the theory. Suggestions for further experimental work are also given.

2. MIXING-ELEMENT ANALYSIS

Essential to the analysis of a frequency converter is a suitable mathematical description of the nonlinear mixing-element (Figure 2-1). Assuming that signal voltages are small compared to those of the pump, it is shown in this chapter that signal voltages and currents are related through a linear differential equation. By considering the harmonic content of the small-signal power that is made available by the mixing action, and by applying the Principle of Harmonic Balance,[7] a solution of the differential equation is later obtained. In general, the solution is in the form of a n by n matrix relating the n voltage harmonics to the n current harmonics. In this work 3 harmonics are considered so that the mathematical description of the mixing-element is in the form of a 3 by 3 matrix.

The mixing-element to be investigated consists of a nonlinear conductance $g(v)$ in parallel with a nonlinear capacitance $C(v)$. These nonlinearities are assumed to be those associated with semiconductor diodes where $g(v)$ is the incremental conductance and $C(v)$ is the junction capacitance. Ohmic losses and series lead inductances* of the diodes are neglected on the understanding that the analysis will be strictly valid only for relatively low frequencies (less than about 150 mc.).

---

* These series components can be accounted for by considering them as part of the terminations.[8]

2.1 Differential Equation of the Mixing-Element

A differential equation relating the signal current $i(t)$ to the signal voltage $v(t)$ of the mixing-element is to be derived (equation 2-10): this equation is used in Section 2.2 to relate voltage and current harmonics. The mixing-element circuit of Figure 2-1 consists of two nonlinear elements with their respective bias and pump voltage sources interconnected in a system of filters. The pump voltages are sinusoidal at frequency f_0. Filters F_0 block frequency f_0 and d-c, but pass all other frequencies. Filters $\overline{F}_0$ pass f_0 and d-c, but block all other frequencies. With this circuit arrangement the signal voltage $v(t)$ and signal current $i(t)$ are influenced by the pump sources only through their action on the nonlinear elements.

From Figure 2-1 the voltage across the nonlinear conductance is

$$V_g(t) = V_{gp}(t) + v(t) \qquad \ldots(2\text{-}1)$$

The signal voltage $v(t)$ is small compared to the pump voltage $V_{gp}(t)$ and therefore the total current $I_g(t)$ through the conductance can be expanded in a two-term Taylor Series.

$$I_g(t) = I\left[V_g(t)\right] = I\left[V_{gp}(t)\right] + g(t)v(t) \qquad \ldots(2\text{-}2)$$

where

$$g(t) = \left.\frac{\partial}{\partial V_g} I\left[V_g\right]\right|_{V_g = V_{gp}(t)} \qquad \ldots(2\text{-}3)$$

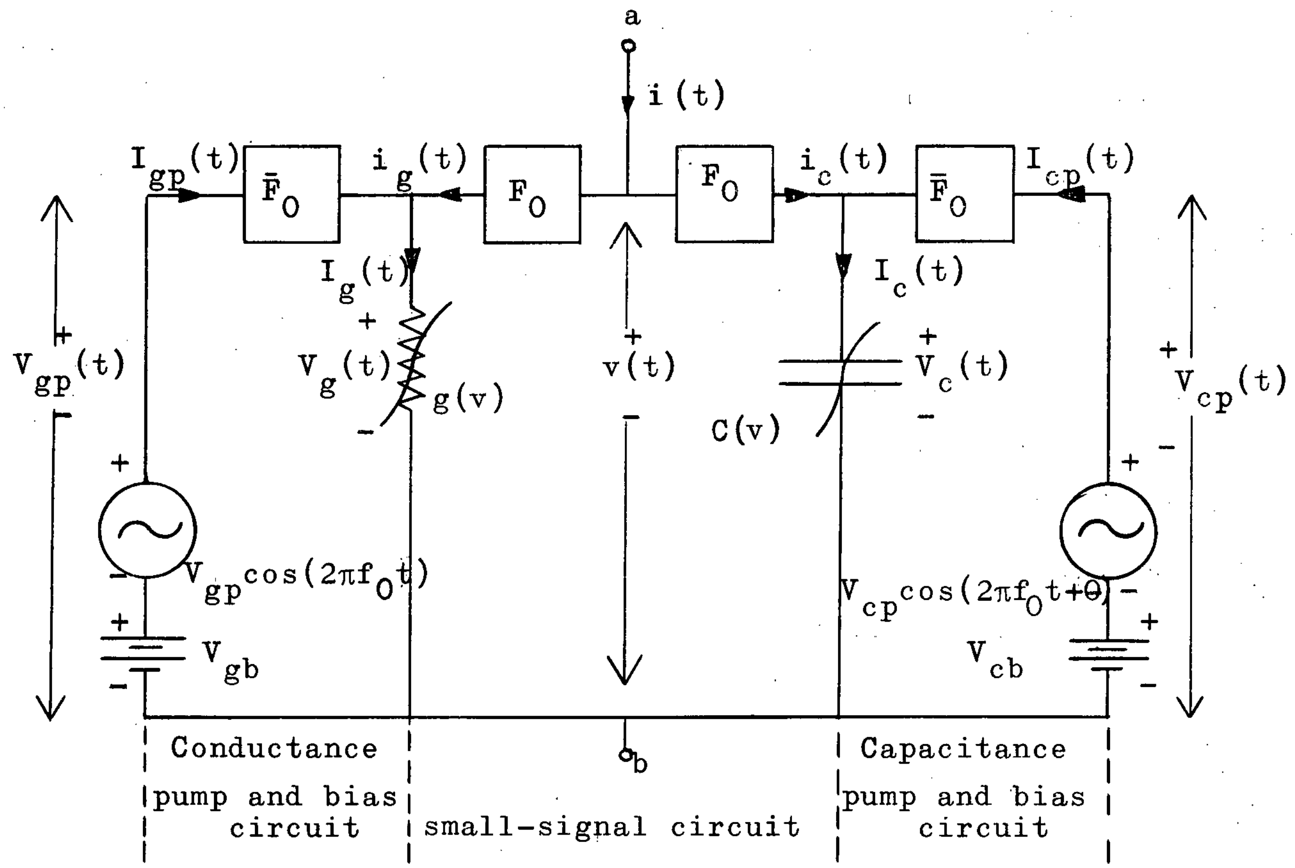

Figure 2-1. Mixing-Element Circuit.

also,

$$I_g(t) = I_{gp}(t) + i_g(t) \qquad \text{...(2-4)}$$

therefore

$$I_{gp}(t) + i_g(t) = I\left[V_{gp}(t)\right] + g(t)v(t) \qquad \text{...(2-5)}$$

This equation can be separated into large and small-signal components,

$$I_{gp}(t) = I\left[V_{gp}(t)\right] \qquad \text{...(2-6)}$$

and

$$i_g(t) = g(t)v(t) \qquad \ldots(2\text{-}7)$$

The small-signal current-voltage relationship for the pumped nonlinear capacitor is derived in a similar manner by expanding the charge on the capacitor in a two-term Taylor Series about the pump voltage. The resulting large and small-signal equations are

$$I_{cp}(t) = \frac{\partial}{\partial t}\, q\left[V_{cp}(t)\right] \qquad \ldots(2\text{-}8)$$

and

$$i_c(t) = \frac{\partial}{\partial t}\left[C(t)v(t)\right] \qquad \ldots(2\text{-}9)$$

The small-signal differential equation relating $v(t)$ and $i(t)$ follow from equations (2-7) and (2-9). Since $i(t) = i_g(t) + i_c(t)$, these equations can be combined to give

$$i(t) = g(t)v(t) + \frac{\partial}{\partial t}\left[C(t)v(t)\right] \qquad \ldots(2\text{-}10)$$

It should be noted that this is a linear differential equation with time varying coefficients. Since this differential equation is linear, the small-signal frequency converter will be a linear device.

2.2 The Mixing-Element Matrix

A solution of differential equation (2-10) under certain assumptions and restrictions is required. It is evident from equation (2-3) that the instantaneous incremental conductance g(t) is a function of the sinusoidal pump voltage $V_{gp}(t)$. Therefore, g(t) is a periodic function of time with fundamental frequency f_0. Since the instantaneous incremental capacitance C(t) is similarly periodic, it follows that both g(t) and C(t) can be expanded in Fourier Series,

$$g(t) = \sum_{n=-\infty}^{n=+\infty} g_n \, e^{jn\omega_0 t} \qquad \ldots(2\text{-}11)$$

and

$$C(t) = \sum_{n=-\infty}^{n=+\infty} C_n' \, e^{jn\omega_0 t} \qquad \ldots(2\text{-}12)$$

where $\omega_0 = 2\pi f_0$

Consider the effect of an input signal $i_2(t)$, at angular frequency ω_2, being applied to the mixing-element (between terminals a-b of Figure 2-1). This signal will "mix" with the components of g(t) and C(t) to produce harmonics at angular frequencies

$$\omega_n = n\,\omega_0 \pm \omega_2 \qquad n = 1, 2, \ldots$$

By terminating the mixing-element properly, power at the various frequencies can be isolated. If terminations are provided such that power can flow only at frequencies given by n = 1, the resulting frequency converter is said to be of the fundamental-mode type.(4) A 3 by 3 matrix for the mixing-element of such a converter will be developed.

Let the angular frequencies at which small-signal power can exist be ω_1, ω_2 and ω_3 where

$$\text{a)} \quad \omega_1 = \omega_0 + \omega_2$$

and ...(2-13)

$$\text{b)} \quad \omega_3 = \omega_0 - \omega_2$$

This frequency spectrum is shown in Figure 2-2.

The small-signal voltage and current can be expressed by the following series;(9)

$$v(t) = \sum_{i=1}^{3} \left(V_i \, e^{j\omega_i t} + V_i^* \, e^{-j\omega_i t} \right) + \text{high-order voltage harmonics} \qquad \text{...(2-14)}$$

$$i(t) = \sum_{i=1}^{3} \left(I_i \, e^{j\omega_i t} + I_i^* \, e^{-j\omega_i t} \right) + \text{high-order current harmonics} \qquad \text{...(2-15)}$$

Since power is restricted to angular frequencies ω_1, ω_2 and ω_3, either the high-order voltage harmonics, or the high-order current harmonics must be absent. Which is absent depends upon

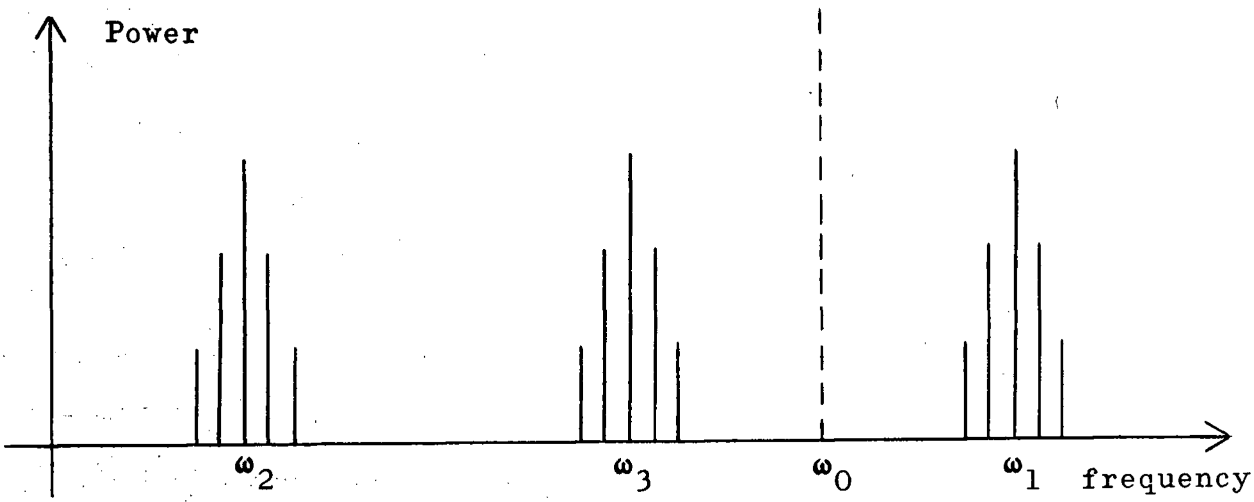

Figure 2-2. Small-Signal Frequency Spectrum.

the terminations of the mixing-element. Substitution of equations (2-11) to (2-15) into equation (2-10) and equating the coefficients of $e^{j\omega_i t}$; i = 1, 2, 3, yields, in matrix form, the equation for the mixing-element.

$$\begin{bmatrix} I_1 \\ I_2 \\ I_3^* \end{bmatrix} = \begin{bmatrix} g_0 + j\omega_1 C_0' & g_1 + j\omega_1 C_1' & g_2 + j\omega_1 C_2' \\ g_{-1} + j\omega_2 C_{-1}' & g_0 + j\omega_2 C_0' & g_1 + j\omega_2 C_1' \\ g_2^* - j\omega_3 C_2'^* & g_1^* - j\omega_3 C_1'^* & g_0^* - j\omega_3 C_0'^* \end{bmatrix} \begin{bmatrix} V_1 \\ V_2 \\ V_3^* \end{bmatrix}$$

...(2-16)

$$\text{or} \quad [I] = [Y]\,[V] \qquad ...(2\text{-}17)$$

In general the off-diagonal Fourier Coefficients of matrix Y are complex. However, with conductance pump voltage as shown in Figure 2-1;

$$V_{gp}(t) = V_{gb} + V_{gp} \cos (\omega_0 t),$$

g(t) is an even function of time with g_n real and $g_n = g_{-n}$. Also for

$$V_{cp}(t) = V_{cb} + V_{cp} \cos (\omega_0 t + \theta),$$

C(t) leads g(t) by θ radians so that C'_n can be replaced by $C_n e^{jn\theta}$ where C_n is real and $C_n = C_{-n}$.

Matrix Y can now be written in terms of real conductance coefficients g_0, g_1 and g_2 and real capacitance coefficients C_0, C_1 and C_2 as follows:

$$\left[Y\right] = \begin{bmatrix} g_0 + j\omega_1 C_0 & g_1 + j\omega C_1 \; e^{j\theta} & g_2 + j\omega_1 C_2 \; e^{j2\theta} \\ g_1 + j\omega_2 C_1 \; e^{-j\theta} & g_0 + j\omega_2 C_0 & g_1 + j\omega_2 C_1 \; e^{j\theta} \\ g_2 - j\omega_3 C_2 \; e^{-j2\theta} & g_1 - j\omega_3 C_1 \; e^{-j\theta} & g_0 - j\omega_3 C_0 \end{bmatrix} \qquad \ldots(2\text{-}18)$$

This mixing-element matrix can be used to analyze the frequency converting properties of a nonlinear conductance, a nonlinear capacitance, or a parallel combination of the two. The 3 by 3 matrix can be reduced to a 2 by 2 matrix by eliminating row i and column i if the converter is terminated so that no power exists at frequency ω_2.

The parameters g_n and C_n are Fourier Coefficients and as such are determined from:

$$g_n = \frac{1}{2\pi}\int_0^{2\pi} g(t)\, e^{-jn\omega_0 t}\, d(\omega_0 t) = g_n(V_{gb}, V_{gp}) \qquad \ldots(2\text{-}19)$$

and

$$C_n = \frac{1}{2\pi}\int_0^{2\pi} C(t)\, e^{-jn(\omega_0 t + \theta)}\, d(\omega_0 t) = C_n(V_{cb}, V_{cp}) \qquad \ldots(2\text{-}20)$$

Curves of $g_n(V_{gb}, V_{gp})$ for tunnel-diodes and of $C_n(V_{cb}, V_{cp})$ for varactor-diodes are obtainable from the literature.[9],[10] The parameters are all positive except g_0 and g_1 of the tunnel-diode which are negative over a limited range of bias and pump voltages V_{gb} and V_{gp} respectively.

3. FREQUENCY CONVERTER ANALYSIS

The mixing-element described by Y-matrix (2-18) is to be used in a unilateral down-converter. In the first section of this chapter a 3-port network equivalent of the mixing-element matrix is defined. The 3-port is reduced to a 2-port and the Y-matrix of the latter network is determined. In the second section, two special cases of the 2-port are considered, and methods by which each case may be made unilateral are outlined.

3.1 Network Representation of the Mixing-Element

Equations (2-16) to (2-18) describe the mixing-element when power at the three frequencies ω_1, ω_2 and ω_3 is allowed to exist. The form of these equations is the same as the nodal equations of a linear 3-port network. The mixing-element can therefore be represented as in Figure 3-1. The signal frequencies at ports 1, 2 and 3 of this network are ω_1, ω_2 and ω_3 respectively.

Using the 3-port equivalent of the mixing-element in a noninverting down-converter,[9] ports 1, 2 and 3 are designated respectively:

(1) r.f. input port

(2) i.f. output port

(3) image port

In subsequent analysis, subscripts 1, 2 and 3 will be associated with the r.f., i.f. and image ports, respectively.

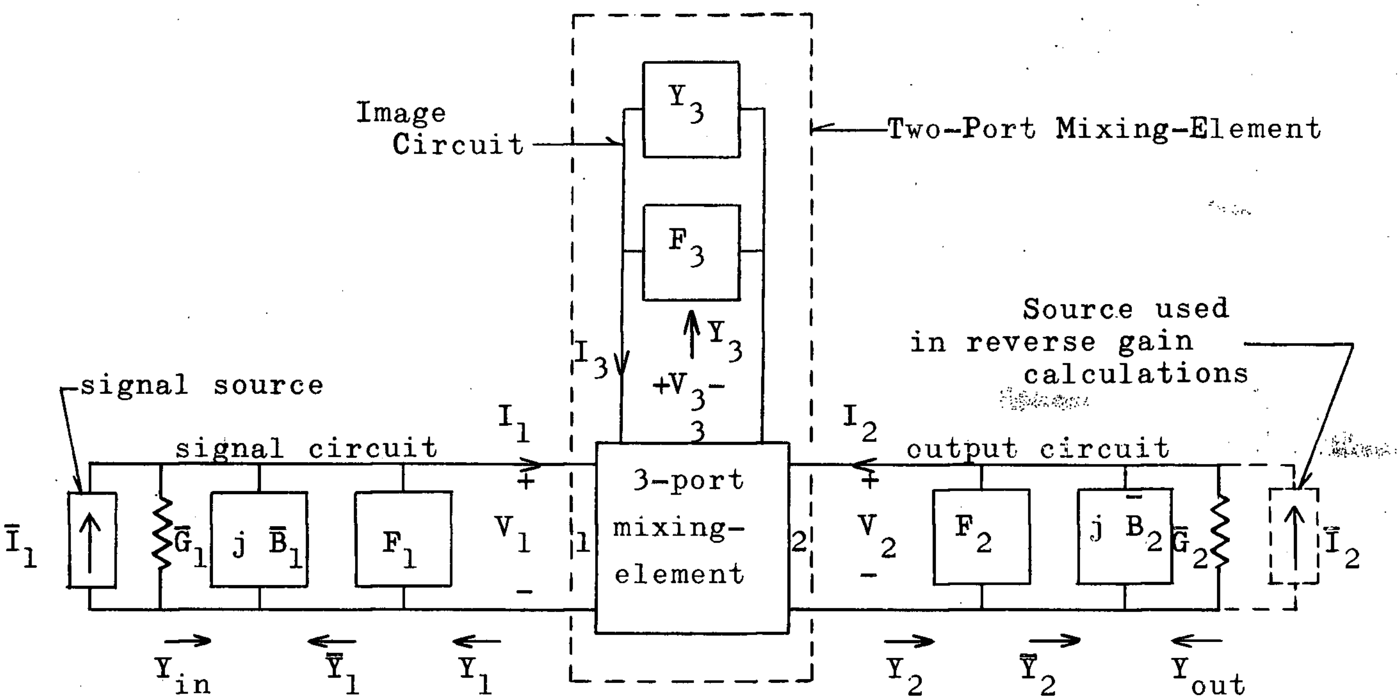

Figure 3-1. Mixing-Element with Terminations.

The 3-port mixing-element (Figure 3-1) can be reduced to the 2-port by terminating the image port with an admittance Y_3.

The 2-port is shown with current sources and terminal admittances as well as the required filters. To be specific, the filters are shown to be of the type that short-circuit high-order voltage harmonics. That is, filter F_i allows only a voltage at frequency ω_i to develop across its terminals.

The equations of the 2-port are obtained from equation (2-16) and matrix (2-18) by eliminating $V_3{}^*$ and $I_3{}^*$

through the relation $I_3^* = -Y_3^* V_3^*$. The equations can be put in the form;

$$\begin{bmatrix} I_1 \\ \\ I_2 \end{bmatrix} = \begin{bmatrix} Y_{11} & Y_{12} \\ \\ Y_{21} & Y_{22} \end{bmatrix} \begin{bmatrix} V_1 \\ \\ V_2 \end{bmatrix} \qquad \ldots(3\text{-}1)$$

where

$$Y_{11} = g_0 + j\omega_1 C_0 - \frac{\left(g_2 + j\omega_1 C_2\, e^{j2\theta}\right)\left(g_2 - j\omega_3 C_2\, e^{-j2\theta}\right)}{Y_3^* + g_0 - j\omega_3 C_0}$$

$$Y_{12} = g_1 + j\omega_1 C_1\, e^{j\theta} - \frac{\left(g_2 + j\omega_1 C_2\, e^{j2\theta}\right)\left(g_1 - j\omega_3 C_1\, e^{-j\theta}\right)}{Y_3^* + g_0 - j\omega_3 C_0}$$

$$Y_{21} = g_1 + j\omega_2 C_1\, e^{-j\theta} - \frac{\left(g_2 - j\omega_3 C_2\, e^{-j2\theta}\right)\left(g_1 + j\omega_2 C_1\, e^{j\theta}\right)}{Y_3^* + g_0 - j\omega_3 C_0}$$

$$Y_{22} = g_0 + j\omega_2 C_0 - \frac{\left(g_1 + j\omega_2 C_1\, e^{j\theta}\right)\left(g_1 - j\omega_3 C_1\, e^{-j\theta}\right)}{Y_3^* + g_0 - j\omega_3 C_0}$$

$$\ldots(3\text{-}2)$$

These parameters are the basis of further analysis.

3.2 Unilateral Frequency Conversion

The frequency converting properties of a converter can be determined from a knowledge of the gain of the device. The transducer gain G_T [13] defined as,

$G_T = \dfrac{\text{power delivered to load}}{\text{available power from source}}$, will be used for this purpose. From this definition the forward gain G_{T12} is given by,

$$G_{T12} = \left. \frac{\left|V_2\right|^2 \bar{G}_2}{\frac{\left|\bar{I}_1\right|^2}{4\bar{G}_1}} \right|_{\bar{I}_2 = 0} = \frac{4\bar{G}_1\bar{G}_2 \left|Y_{21}\right|^2}{\left|\left(Y_1 + Y_{11}\right)\left(Y_2 + Y_{22}\right) - Y_{12}Y_{12}\right|^2}$$

...(3-3)

and the reverse gain G_{T21} by

$$G_{T21} = \left. \frac{\left|V_1\right|^2 \bar{G}_1}{\frac{\left|\bar{I}_2\right|^2}{4\bar{G}_2}} \right|_{\bar{I}_1 = 0} = \frac{4\bar{G}_1\bar{G}_2 \left|Y_{12}\right|^2}{\left|\left(Y_1 + Y_{11}\right)\left(Y_2 + Y_{22}\right) - Y_{12}Y_{21}\right|^2}$$

...(3-4)

For a unilateral down-converter G_{T21} is zero and G_{T12} is finite. This implies that $Y_{12} = 0$ and $Y_{21} \neq 0$.

From Y-parameters (3-2) two methods of obtaining unilateral down-conversion are placed in evidence.

Method I. Quadrature Pumping

This method, applicable in particular to converters with a short-circuit image termination ($Y_3 = \infty$), depends upon proper choice of the pump phase angle Θ.

With $Y_3 = \infty$ the Y matrix of equation (3-1) becomes:

$$\begin{bmatrix} Y_{11} & Y_{12} \\ Y_{21} & Y_{22} \end{bmatrix} = \begin{bmatrix} g_0 + j\omega_1 C_0 & g_1 + j\omega_1 C_1 \; e^{j\theta} \\ g_1 + j\omega_2 C_1 \; e^{-j\theta} & g_0 + j\omega_2 C_0 \end{bmatrix} \qquad \ldots(3\text{-}5)$$

For unilateral gain

$$Y_{12} = g_1 + j\omega_1 C_1 \; e^{j\theta} = 0.$$

Therefore, if 1. $\theta = \pm \frac{\pi}{2}$ radians

and

2. $g_1 \mp \omega_1 C_1 = 0$

the converter will be unilateral. Since θ is the phase angle by which the capacitance pump voltage leads the conductance pump voltage, the two nonlinear elements must be pumped in time quadrature.* This condition can only be satisfied if the two nonlinear elements are physically separate, i.e., not joined directly together as is the case for the nonlinear conductance and the nonlinear capacitance of a single tunnel-diode.

The unilateral feature obtained from this method is present only at the band-centre frequency since the balance

---

* The theory of unilateral frequency conversion by the quadrature pumping method, for a crystal-diode and a varactor-diode used as an up-converter, has been outlined in the literature.(11),(12) The method can equally well be applied to a tunnel-diode and a varactor-diode for which unilateral down-conversion with gain is possible.

required by condition 2 above can only be satisfied at one frequency.

Method II. Image Termination

This method for obtaining unilateral down-conversion depends upon proper choice of the image termination Y_3. The case in which $\theta = 0$ will be discussed in detail since for this case the nonlinear conductance and the nonlinear capacitance can be that of a single tunnel-diode.

The Y-parameters, for $\theta = 0$, from equations (3-2) become:

$$Y_{11} = g_0 + j\omega_1 C_0 - \frac{\left(g_2 + j\omega_1 C_2\right)\left(g_2 - j\omega_3 C_2\right)}{Y_3^* + g_0 - j\omega_3 C_0}$$

$$Y_{12} = g_1 + j\omega_1 C_1 - \frac{\left(g_2 + j\omega_1 C_2\right)\left(g_1 - j\omega_3 C_1\right)}{Y_3^* + g_0 - j\omega_3 C_0}$$

$$Y_{21} = g_1 + j\omega_2 C_1 - \frac{\left(g_2 - j\omega_3 C_2\right)\left(g_1 + j\omega_2 C_1\right)}{Y_3^* + g_0 - j\omega_3 C_0}$$

$$Y_{22} = g_0 + j\omega_2 C_0 - \frac{\left(g_1 + j\omega_2 C_1\right)\left(g_1 - j\omega_3 C_1\right)}{Y_3^* + g_0 - j\omega_3 C_0}$$

...(3-6)

The down-converter will be unilateral provided:

$$Y_{12} = g_1 + j\omega_1 C_1 - \frac{\left(g_2 + j\omega_1 C_2\right)\left(g_1 - j\omega_3 C_1\right)}{Y_3^* + g_0 - j\omega_3 C_0} = 0$$

The image termination Y_3 required to satisfy this identity is:

$$Y_3 = -g_0 - j\omega_3 C_0 + \frac{\left(g_2 - j\omega_1 C_2\right)\left(g_1 + j\omega_3 C_1\right)}{g_1 - j\omega_1 C_1} \qquad \text{...(3-7)}$$

This particular image termination gives unilateral down-conversion.

Y_3 can be realized, and equation (3-7) satisfied, for the case where the capacitance terms are zero: but both Y_{12} and Y_{21} vanish simultaneously. Capacitance terms as well as conductance terms are essential for unilateral conversion using this method.

When the g and C parameters that make up Y_3 are those of pumped semiconductor diodes it can be shown that Y_3 cannot be a positive real driving-point admittance, (see Appendix I). With tunnel-diode g parameters the real part of Y_3 can be positive (Section 4.2b) so that Y_3 can be approximated with linear passive elements. Since the admittance can only be approximated, unilateral gain by this method, as for the quadrature pumped converter, can only be obtained at the band-centre frequency. The parallel combination of a resistor and a capacitor is a close enough approximation to Y_3 to give 20 db. of rejection over a 5% bandwidth (Section 4.5).

It is possible to explain the inherent narrow-band feature of the quadrature and image termination methods. Roughly speaking, these methods depend upon the reverse gain due to the conductance element to cancel that due to the capacitance element. For this condition, a net forward gain still exists because the forward and reverse gains due to the capacitance are not equal.[14] The gain provided by the conductance is frequency independent[4] whereas that of the capacitance is frequency dependent.[9] Hence the balance required for the unilateral feature can only be obtained at one frequency. For the quadrature pumped converter one cannot, by altering the terminations, overcome this basic limitation; whereas, for the image-terminated converter, zero reverse gain can be obtained over as large a bandwidth as the Y_3 of equation (3-7) can be synthesized.

4. UNILATERAL DOWN-CONVERSION BY THE IMAGE TERMINATION METHOD

The first portion of this chapter is devoted to the study of a converter with optimum terminations (Sections 4.2 to 4.4). Such terminations can be realized only with an infinite number of elements, but they enable the theoretical study of the converter to be made under the best possible conditions. Such topics as gain and stability are considered. In the last part of this chapter, a more practical converter with simple terminations is discussed. A model of this converter was analyzed on the computer in order to obtain frequency response curves.

4.1 Approximations

The 2-port Y-parameters (equations 3-6) are applicable to an image terminated converter in which the nonlinear conductance and nonlinear capacitance are directly in parallel. For the frequency range being considered and the nonlinear capacitance that of a semiconductor diode, it is found that C_2 can be neglected (Section 6.1). Under the following assumption and definitions,

$$C_2 = 0$$

$$\alpha \triangleq \frac{\omega_0 C_1}{g_1} \quad \text{(nonlinearity factor)}$$

$$\beta \triangleq \frac{\omega_0 C_0}{g_0} \quad \text{(loading factor)}$$

$$\Omega_1 \triangleq \frac{\omega_1}{\omega_0} \quad \text{(normalized frequency)} \qquad \ldots(4\text{-}1)$$

$$\Omega_2 \triangleq \frac{\omega_2}{\omega_0} \quad (\quad " \qquad " \quad)$$

$$\Omega_3 \triangleq \frac{\omega_3}{\omega_0} \quad (\quad " \qquad " \quad)$$

the Y parameters of (3-6) can be written in the following simplified form:

$$
\begin{aligned}
Y_{11} &= g_0(1 + j\Omega_1\beta) - \frac{g_2{}^2}{Y_3{}^* + g_0(1 - j\Omega_3\beta)} \\
Y_{12} &= g_1(1 + j\Omega_1\alpha) - \frac{g_1 g_2(1 - j\Omega_3\alpha)}{Y_3{}^* + g_0(1 - j\Omega_3\beta)} \\
Y_{21} &= g_1(1 + j\Omega_2\alpha) - \frac{g_1 g_2(1 + j\Omega_2\alpha)}{Y_3{}^* + g_0(1 - j\Omega_3\beta)} \qquad \ldots(4\text{-}2) \\
Y_{22} &= g_0(1 + j\Omega_2\beta) - \frac{g_1{}^2(1 + j\Omega_2\alpha)(1 - j\Omega_3\alpha)}{Y_3{}^* + g_0(1 - j\Omega_3\beta)}
\end{aligned}
$$

These parameters will be used as the basis for analysis of the image terminated converter.

4.2 Optimum Terminations

A unilateral down-converter that has the following properties will be considered to have optimum terminations.

a) No r.f., i.f. or image attenuation due to filters.

b) Wide-band unilateral behaviour with a passive image termination.

c) Input and output admittance real over a wide band.

a) Optimum Filters

It is assumed that the filters F_1, F_2 and F_3, (Figure 3-1) give zero attenuation and zero phase shift over wide pass-bands centredaround their respective centre frequencies, that is, $\overline{Y}_i = Y_i$ over a wide band. These filters will be termed optimum. In addition,it is assumed that filter F_i presents infinite admittance to signals at frequencies other than f_i.

This latter assumption has been implicitly assumed in the derivation of the mixing-element matrix equations (2-16) to (2-18).

b) Optimum Image Termination

Consideration of equations (3-7) and (4-1) reveals that if

$$Y_3 = -g_0(1 + j\Omega_3\beta) + g_2 \frac{(1 + j\Omega_3\alpha)}{1 - j\Omega_1\alpha} \qquad \ldots(4\text{-}3)$$

the down-converter will be unilateral for all frequencies. Y_3 is not a positive real driving-point admittance and therefore cannot be realized exactly. For a converter with optimum terminations it is assumed, however, that the approximation to Y_3 is very close over a wide frequency band.

For Y_3 to be a passive termination it is necessary that $\mathrm{Re}\left(Y_3\right) \geq 0$. From the expansion of Y_3 it follows that $\mathrm{Re}\left(Y_3\right) \geq 0$ for

$$\frac{g_0}{g_2} \leq 1 - \frac{2\Omega_1\alpha^2}{1 + \Omega_1{}^2\alpha^2} \qquad \ldots(4\text{-}4)$$

The equality of (4-4) is plotted in Figure 4-1 as a function of Ω_1 with α as a parameter.

The $\mathrm{Re}\left(Y_3\right)$ will be positive for a given α only if $\frac{g_0}{g_2}$ is less than the value given by the graph. For a crystal-

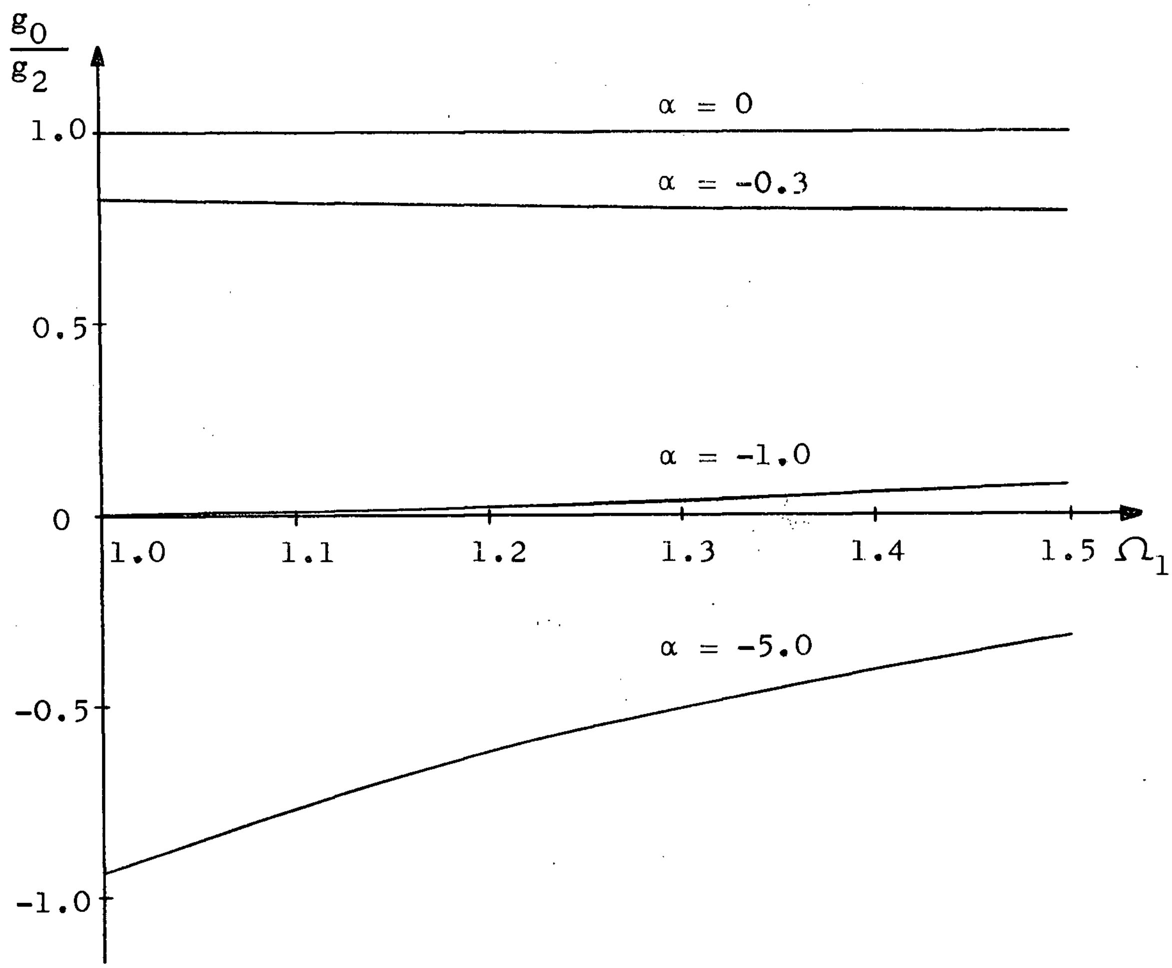

Figure 4-1. Boundaries of a Passive Image Termination ($\mathrm{Re}\left(Y_3\right) = 0$).

diode it can be shown[1] that $\frac{g_0}{g_2} \geq 1$. This rules out the possible use of such a diode to achieve unilateral conversion with a passive image termination. A tunnel-diode, however, can satisfy condition 4-4 over a region of its characteristic curve.[10] Further analysis will therefore be carried out on the understanding that the required g parameters are those of a tunnel-diode.

c) Optimum Input and Output Terminations

The input and output admittances are made real by suitably choosing $\overline{B}_1$ and $\overline{B}_2$ respectively. From Figure 3-1 it follows that with optimum filters;

$$Y_{in} = Y_{11} - \frac{Y_{12}Y_{21}}{Y_{22} + Y_2} + j\,\overline{B}_1 \qquad \text{...(4-5)}$$

and

$$Y_{out} = Y_{22} - \frac{Y_{12}Y_{21}}{Y_{11} + Y_1} + j\,\overline{B}_2 \qquad \text{...(4-6)}$$

Since $Y_{12} = 0$, by choice of Y_3, the input and output admittances will be real if

$$\overline{B}_1 = -I_m\left(Y_{11}\right) = \frac{2\;g_2\alpha}{1 + \Omega_3{}^2\alpha^2} - \Omega_1\beta g_0 \qquad \text{...(4-7)}$$

and

$$\overline{B}_2 = -I_m\left(Y_{22}\right) = \frac{g_1{}^2\alpha}{g_2}\left(\Omega_1 + \Omega_2\right) - \Omega_2\beta g_0 \qquad \text{...(4-8)}$$

For the optimum terminations and filters defined in a, b and c above, the converter equations, from equations (4-2), become;

$$\begin{bmatrix} \bar{I}_1 \\ \\ 0 \end{bmatrix} = \begin{bmatrix} \bar{G}_1 + g_0 - g_2\left(\dfrac{1 - \Omega_1\Omega_3\alpha^2}{1 + \Omega_3{}^2\alpha^2}\right) & 0 \\ \\ -j\ 2\ g_1\alpha \left(\dfrac{1 + j\Omega_2\alpha}{1 - j\Omega_3\alpha}\right) & \bar{G}_2 + g_0 - \dfrac{g_1{}^2}{g_2}\left(1 - \Omega_1\Omega_2\alpha^2\right) \end{bmatrix} \begin{bmatrix} V_1 \\ \\ V_2 \end{bmatrix} \qquad \ldots(4\text{-}9)$$

It should be noted that Y_3, $\bar{B}_1$, and $\bar{B}_2$ are all impossible to realize with a finite number of passive elements. The converter with optimum terminations is still of interest since the terminations can be synthesized theoretically to any required degree of accuracy. Also, the band-centre characteristics of a converter with simple terminations can equal those with optimum terminations, (Section 4.5).

4.3 Converter Stability

It has been established (Section 4.2b) that the g parameters of a tunnel-diode, in conjunction with a passive image termination, are suitable for unilateral down-conversion. Since spurious oscillations are difficult to avoid in circuits employing tunnel-diodes[15] the converter stability conditions are of prime importance.

With reference to the 2-port network of Figure 3-1, necessary conditions for stability are:[16]

$$\begin{aligned} &(1)\quad \bar{G}_1 + \mathrm{Re}\left(Y_{in}\right) > 0 \\ &(2)\quad \bar{G}_2 + \mathrm{Re}\left(Y_{out}\right) > 0 \end{aligned} \qquad \ldots(4\text{-}10)$$

For a converter with optimum terminations and filters,

Y_{in} and Y_{out} are real, and have values G_{in} and G_{out} given by equations (4-5), (4-6) and (4-9).

$$G_{in} = g_0 - g_2 \left(\frac{1 - \Omega_1 \Omega_3 \alpha^2}{1 + \Omega_3^{\,2} \alpha^2}\right) = g_0 - g_2 \left(1 - \frac{2(2 - \Omega_1)\alpha^2}{1 + (2 - \Omega_1)^2 \alpha^2}\right) \qquad \ldots(4\text{-}11)$$

$$G_{out} = g_0 - \frac{g_1^{\,2}}{g_2}\left(1 - \Omega_1 \Omega_2 \alpha^2\right) = g_0 - \frac{g_1^{\,2}}{g_2}\left(1 - (\Omega_1 - 1)\ \Omega_1 \alpha^2\right) \qquad \ldots(4\text{-}12)$$

These functions are plotted in Figure 4-2 for a particular set of g and α parameters.* Both G_{in} and G_{out} are predominantly negative. From (4-10), the converter will be stable if

$$\bar{G}_1 + G_{in} > 0$$

and $\qquad \ldots(4\text{-}13)$

$$\bar{G}_2 + G_{out} > 0$$

for all values of frequency.

---

* The g parameters chosen, namely $g_0 = -4\ m\Omega^{-1}$, $G_1 = -2\ m\Omega^{-1}$ and $g_2 = 2\ m\Omega^{-1}$ are approximately those of a 1 ma. germanium tunnel-diode biased at the point where g(v) is a minimum and pumped with a 100 mv. peak to peak source. This mode of operation satisfies the condition $\frac{g_0}{g_2} \leq 1$ (equation 4-4) and provides conversion gain with source and load resistances within the common range of 50 to 300 ohms. These g parameters are used in further illustrative graphs in this chapter.

For these operating conditions the nonlinear capacitance of the tunnel diode is sufficient to give values of α between about 0 and -1.0 for pump frequencies less than about 150 mc. Values of α less than -1.0 correspond to pumped elements consisting of a tunnel-diode in parallel with a varactor-diode.

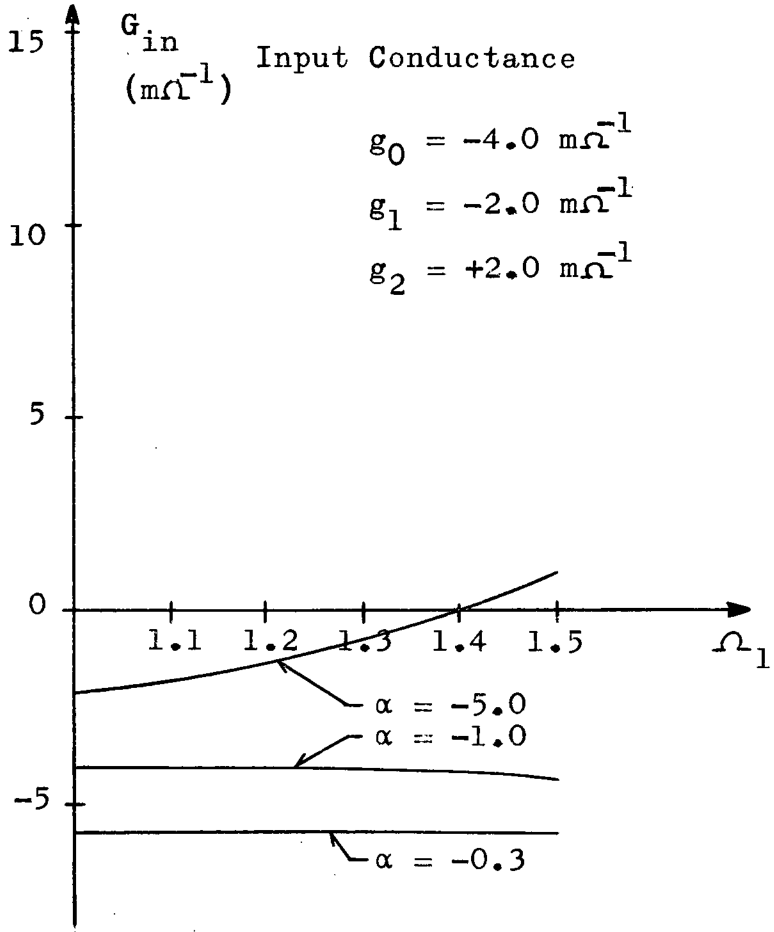

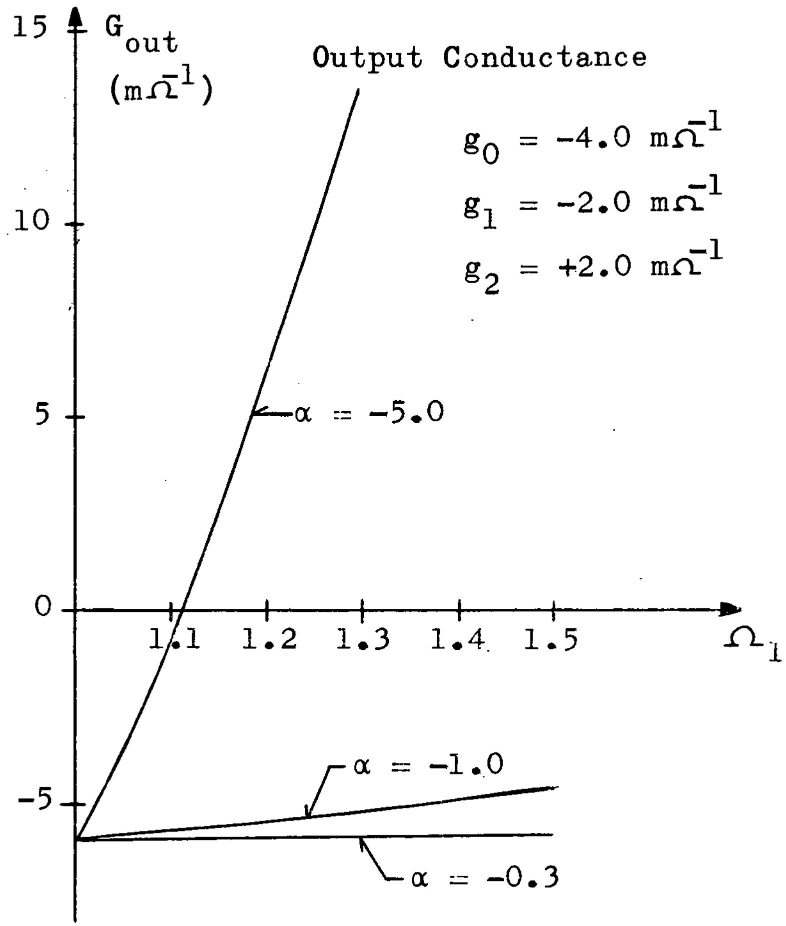

Figure 4-2. Input and Output Conductance vs. Normalized Input Frequency

4.4 Gain With Optimum Terminations

From equations (3-3) and (4-9) the forward gain of the converter with optimum terminations becomes;

$$G_{T12} = \frac{16\,\bar{G}_1\bar{G}_2\,g_1^{\,2}\alpha^2 \left|\dfrac{1 + j\Omega_2\alpha}{1 - j\Omega_3\alpha}\right|^2}{\left|\left\{\bar{G}_1 + g_0 - g_2\left(\dfrac{1 - \Omega_1\Omega_3\alpha^2}{1 + \Omega_3^{\,2}\alpha^2}\right)\right\}\left\{\bar{G}_2 + g_0 - \dfrac{g_1^{\,2}}{g_2}\left(1 - \Omega_1\Omega_2\alpha^2\right)\right\}\right|^2} \quad \ldots(4\text{-}14)$$

The denominator of this expression is of the form

$$\left|\left(\bar{G}_1 + G_{in}\right)\left(\bar{G}_2 + G_{out}\right)\right|^2 ,$$

which upon comparison with the stability conditions (equations 4-13) is seen to approach zero when instability occurs. That is, the condition for infinite gain is the same as the conditions for instability. With such a device any reasonable value of gain can be realized by choice of $\bar{G}_1$ and $\bar{G}_2$, but high gain is obtained at the expense of stability.

Variation of forward gain G_{T12} with frequency for particular values of source and load conductances $\bar{G}_1$ and $\bar{G}_2$ respectively, (both 8 mΩ^{-1}) is shown in Figure 4-3. Only for $|\alpha|$ large is the gain significantly frequency dependent. The reverse gain G_{T21} of a converter with these terminations is defined to be zero.

A set of three equal-gain contour curves in the

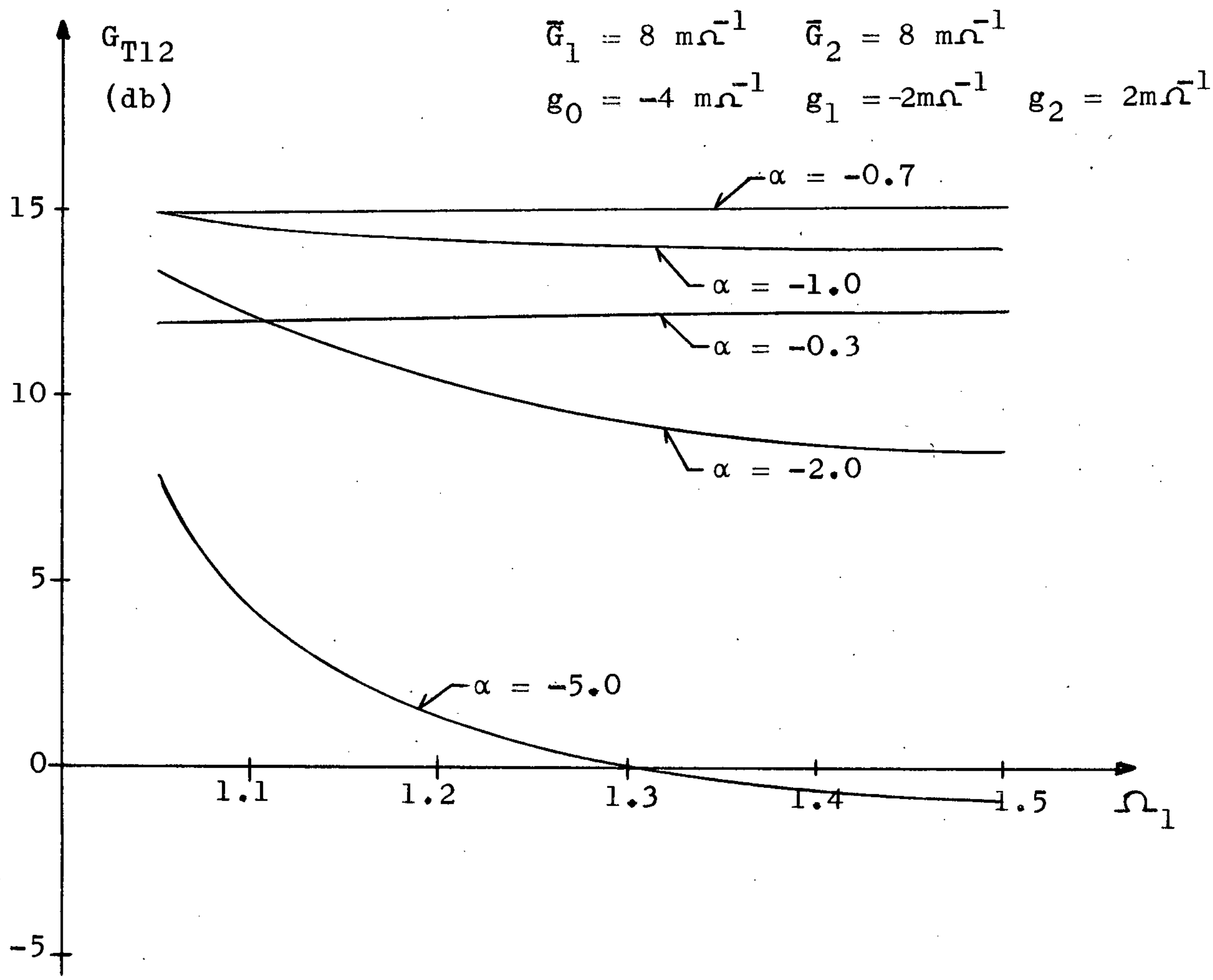

Figure 4-3. Forward Gain with Optimum Terminations vs. Normalized Input Frequency.

$\bar{G}_1 - \bar{G}_2$ plane corresponding to three values of α with $\Omega_1 = 1.25$ is given in Figure 4-4. For $\alpha = -.3$ and -1.0 both G_{in} and G_{out} are negative, but for $\alpha = -5.0$ G_{in} is negative and G_{out} positive: consequently the curves for $\alpha = -5.0$ are of a different form. Since G_{T12} is practically independent of Ω_1 for $\alpha = -.3$ and -1.0 the contours corresponding to these values are approximately valid for all values of Ω_1.

4.5 Frequency Characteristics of a Computer Analyzed Model with "Practical Terminations"

The optimum filters and terminations specified in Section 4.2 cannot be realized practically. One step closer towards the practical case is provided by simple passive-element terminations (Figure 4-5 elements with superscript bars) and antiresonant frequency filtering (L_{if}, C_{if}). The filtering by the latter components is assumed adequate to suppress unwanted harmonics in the sense described for optimum filters (Section 4.2a). This assumption is only violated when L_{if}/C_{if} is a very high ratio.

The equations for this converter are based upon the mixing-element parameters (4-2). The terminating and filter components for this "practical" converter are chosen to give the same loading, at band-centre, as optimum terminations (Section 4.2). By choosing the components in this manner, the characteristics of the converter at band-centre are the same as those obtained with optimum terminations. The terminating component values are given in Appendix II.

A converter with terminating and filter components as described (Figure 4-5) was analyzed on the digital computer.

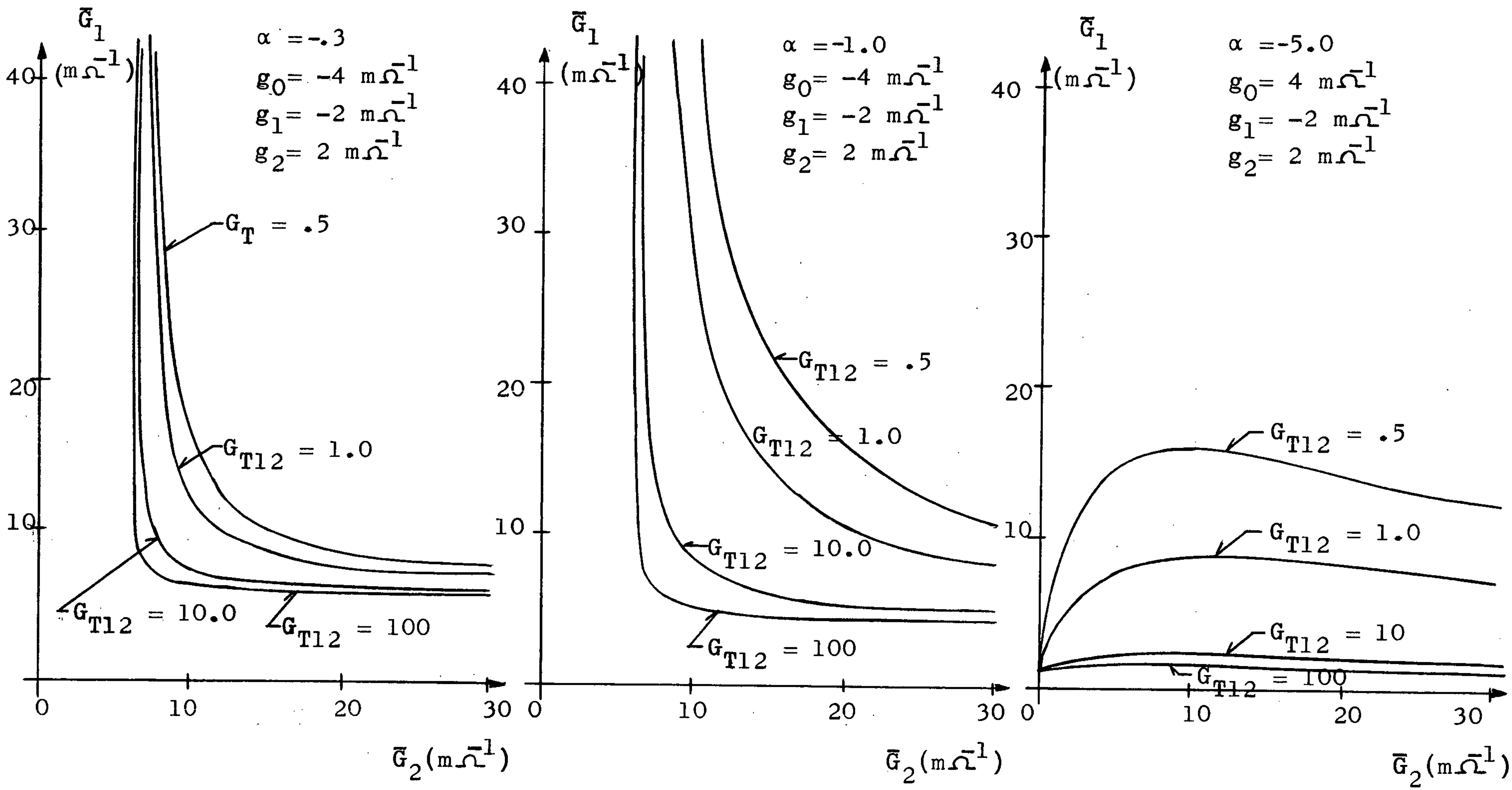

Figure 4-4. Equal-Gain Contours of Converter with Optimum Terminations

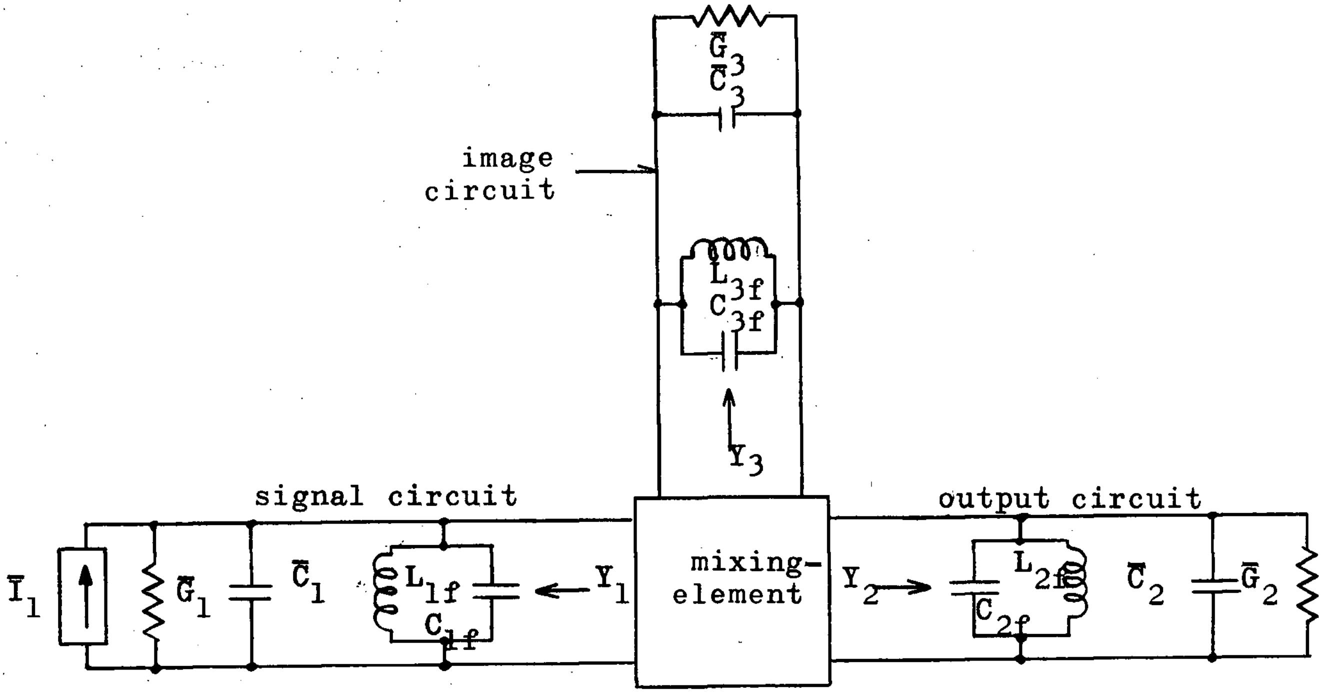

Figure 4-5. Mixing-Element with Practical Terminations.

Frequency responses based on the forward and reverse gain equations (3-3) and (3-4) respectively, were obtained for various L_{if}/C_{if} ratios and values of α. These are shown in Figures 4-6. For small L_{if}/C_{if} ratios the bandwidth is very narrow. As the ratio is increased the bandwidth increases: the upper limit to the bandwidth is set by the necessity to channel power at the desired frequencies. The curves of Figure 4-6 for largest bandwidth could be realized by using additional frequency filtering. The L_{if}/C_{if} ratio to which they correspond is large, and thus violates the assumption stated in the first paragraph of this section.

The reverse gain "bandwidth" seems to be practically independent of the L_{if}/C_{if} ratio, indicating that this "bandwidth" is limited by the approximate image termination. The narrow reverse gain "bandwidth" probably has repercussions in the critical tuning of the experimental converter, (Section 6.2). The response is not greatly affected by α (a measure of the nonlinear capacitance), even though the unilateral property depends upon this capacitance. Thus, there is little to be gained at these frequencies by increasing the effective nonlinear capacitance of a tunnel-diode by bridging it, for example, with a varactor-diode.

In addition to the response curves of Figure 4-6, the gain contours of Figure 4-4 are also applicable at band-centre to the converter with practical terminations. Thus, the mid-band gains of Figure 4-6, for which $\bar{G}_1 = 8m\Omega^{-1}$ and $\bar{G}_2 = 8m\Omega^{-1}$, can also be obtained from Figure 4-4.

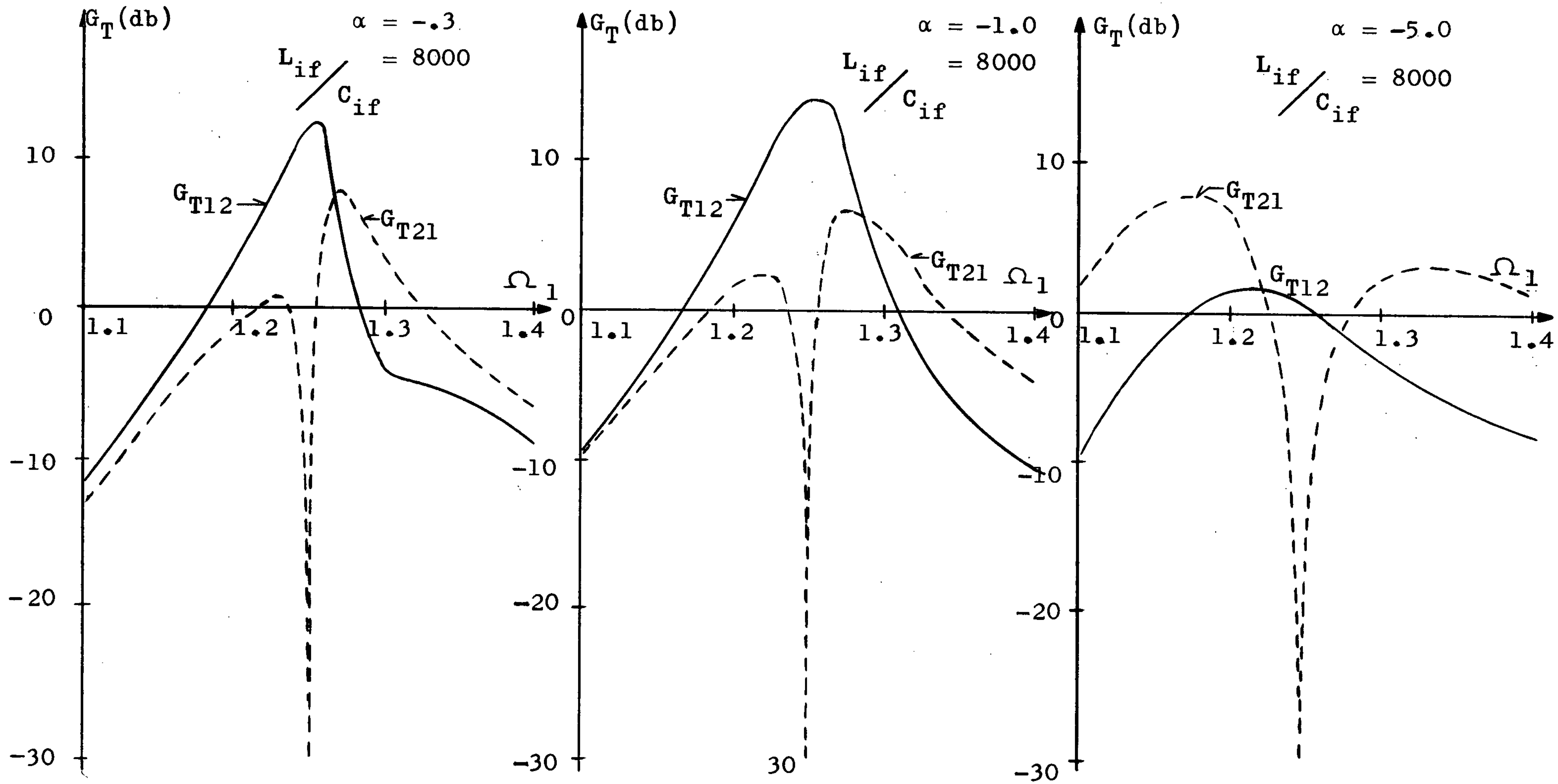

($\bar{G}_1 = 8\ m\Omega^{-1}$, $\bar{G}_2 = 8\ m\Omega^{-1}$, $\beta = -.75$, $g_0 = -4\ m\Omega^{-1}$, $g_1 = -2\ m\Omega^{-1}$, $g_2 = 2\ m\Omega^{-1}$)

Figure 4-6(a). Forward and Reverse Gain of a Converter with Practical Terminations.

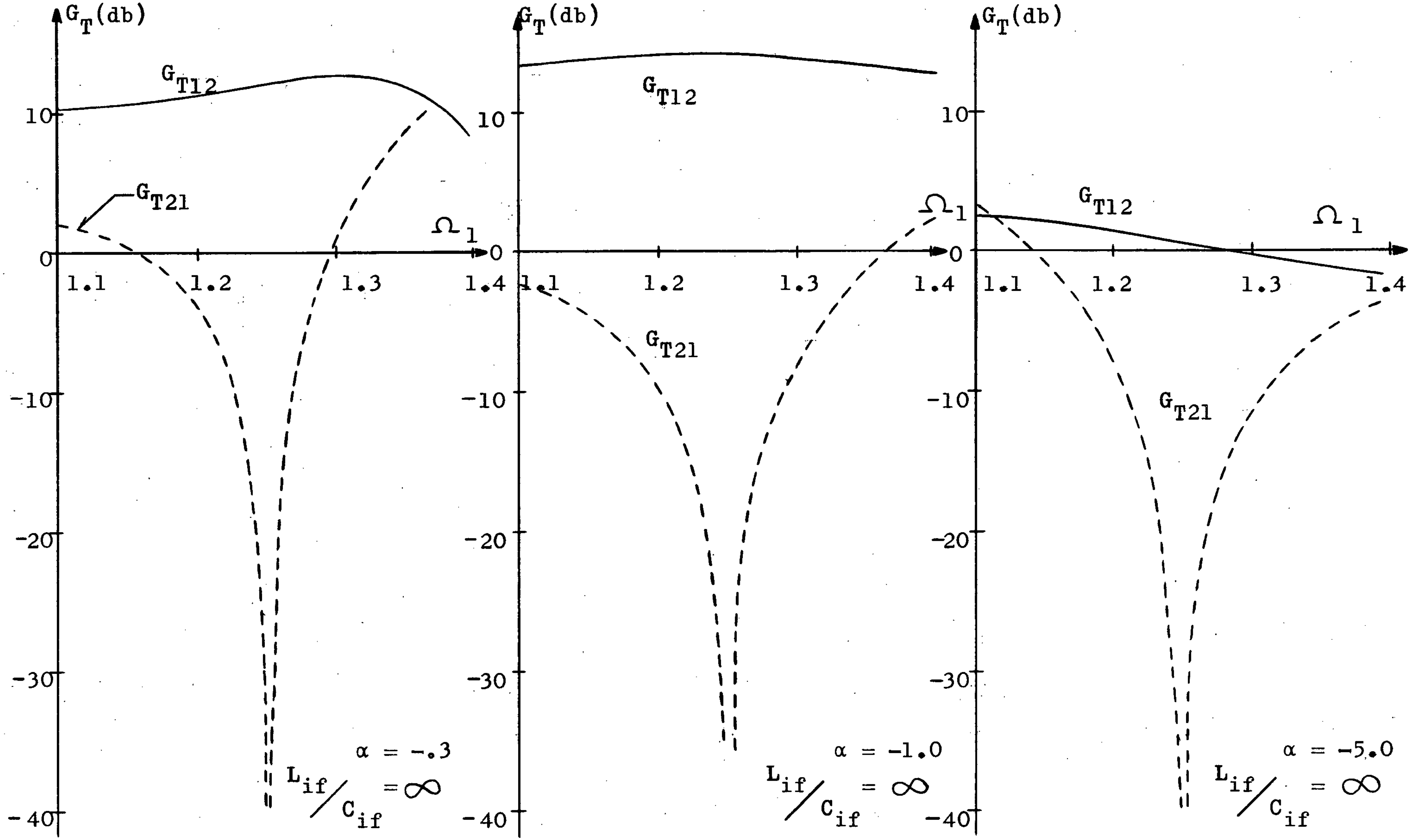

$(\overline{G}_1 = 8\ m\Omega^{-1},\ \overline{G}_2 = 8\ m\Omega^{-1},\ \beta = -.75,\ g_0 = -4\ m\Omega^{-1},\ g_1 = -2\ m\Omega^{-1},\ g_2 = 2\ m\Omega^{-1})$

Figure 4-6(b). Forward and Reverse Gain of a Converter with Practical Terminations.

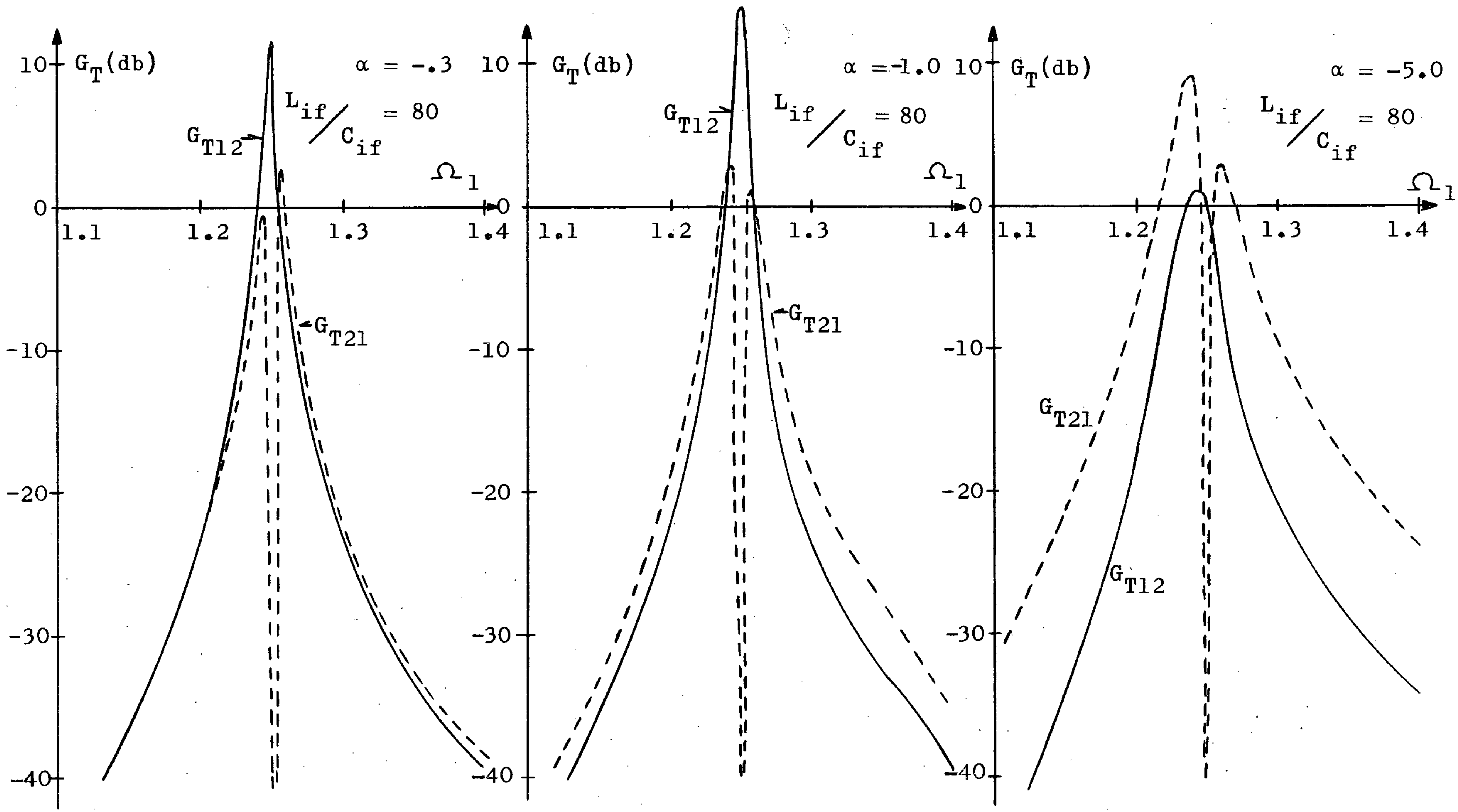

($\bar{G}_1 = 8$ mΩ^{-1}, $\bar{G}_2 = 8$ mΩ^{-1}, $\beta = -.75$, $g_0 = -4$ mΩ^{-1}, $g_1 = -2$ mΩ^{-1}, $g_2 = 2$ mΩ^{-1})

Figure 4-6(c). Forward and Reverse Gain of a Converter with Practical Terminations.

5. NOISE

The very important topic of noise performance has not been studied experimentally. The noise at the output is due to two sources: the signal source and the equivalent diode noise; and the image circuit noise. From Kim,[8] a limiting figure for the first source of noise is given by

$$F = 1 + \frac{G_0}{\overline{G}_1} \qquad \text{where } G_0 = \text{equivalent shot noise conductance.}$$

For the experimental diode, $G_0 = 10\ \mathrm{m}\Omega^{-1}$ and $\overline{G}_1 = 10\ \mathrm{m}\Omega^{-1}$; $F = 3$ db. Additional noise due to the image circuit can be represented by a conductance across the output terminals. The value of this conductance, based on an estimated power gain of unity between image and output circuits, is $\overline{G}_3$ $(2\ \mathrm{m}\Omega^{-1})$. Kim's noise figure now becomes;

$$F = 1 + \frac{G_0}{\overline{G}_1} + \frac{G_3}{\overline{G}_1} \quad \text{and has a value } F = 3.4 \text{ db.}$$

These noise calculations, based on Kim's limiting noise figure expression, indicate that the noise performance of the unilateral converter is slightly poorer than the bilateral converter. This result can be reversed if the converter feeds into a circuit producing noise power across its input terminals; (e.g. a transistor). In such a case, the noise at the input of the bilateral converter is increased by feedback; and the overall noise figure can be greater than that with the unilateral converter.

6. EXPERIMENTAL

An experimental study was undertaken in order to verify the unilateral property set forth in the theory. With this in mind, a 127 mc. to 27 mc. converter utilizing the nonlinear conductance and the nonlinear capacitance of a single tunnel-diode was constructed.

6.1 Experimental Converter Circuit and Its Elements

The circuit chosen for experimental work is shown in Figure 6-1. Before considering this circuit in detail, it is worthwhile to examine the characteristics and equivalent circuit of the GE IN 2939 tunnel-diode used. These are shown in Figure 6-2.

In theory it was found that a bias point at or near the minimum value of the conductance g(v) is desirable.* From the manufacturers' specifications and from experimental measurement, the conductance and the capacitance at this bias point are approximately $-6.6\ m\Omega^{-1}$ and 12 p.f. respectively. For these values, the series resistance $R_s = 1\Omega$ and the series inductance $L_s \cong 5$ n.h. are negligible at frequencies below the r.f. frequency of 127 mc. This fact had been previously assumed in the theory.

A 100 mc. pump source effects the variation of the conductance and capacitance. For a pump voltage of 100 mv. peak to peak across the diode, theoretical values of the fundamental, the first and second harmonics of the time varying

---

* For example, footnote of Section 4.3.

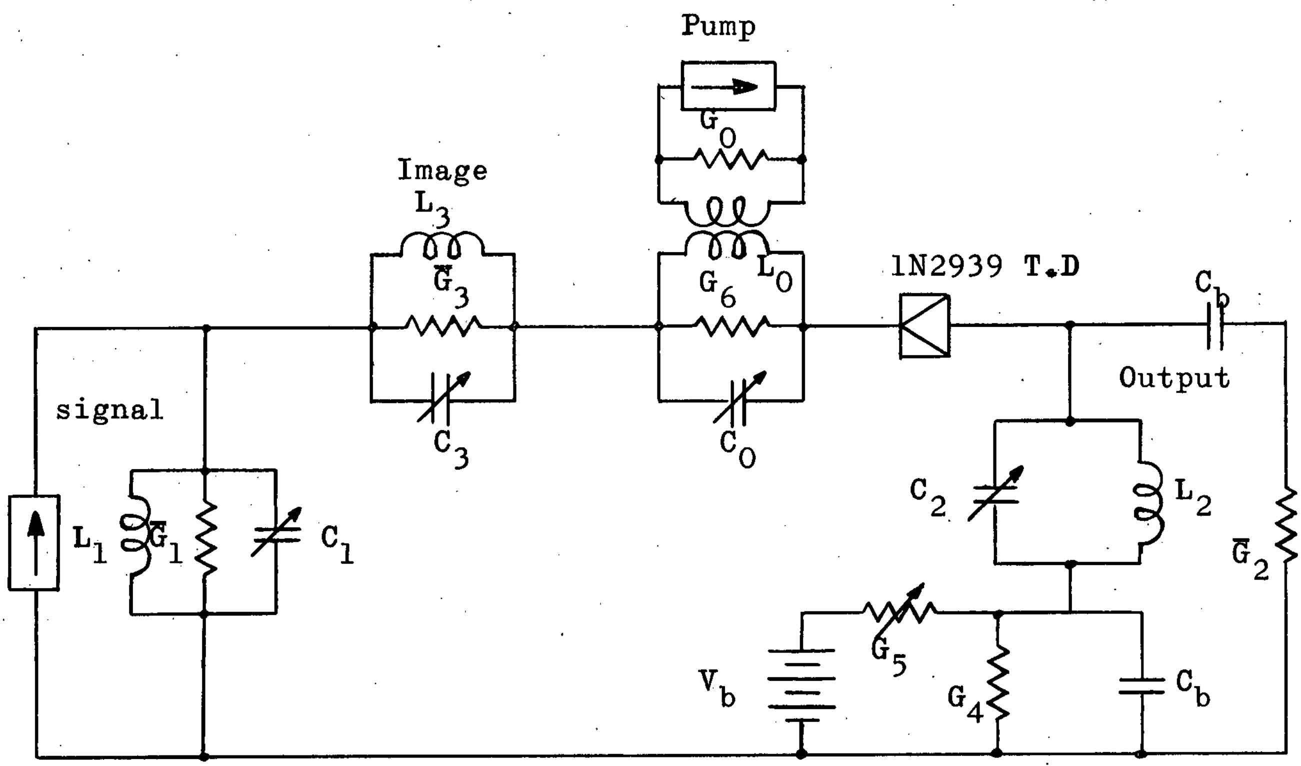

Pump frequency 100 mc   Signal frequency 127 mc

Output frequency 27 mc   Image frequency 73 mc

$G_0 = 20m\Omega^{-1}$, $\bar{G}_1 = 10m\Omega^{-1}$, $\bar{G}_2 = 10m\Omega^{-1}$,

$\bar{G}_3 = 2m\Omega^{-1}$, $G_6 = 200m\Omega^{-1}$, $L_1 \simeq .05$ μ.h.,

$L_2 \simeq .2$ μ.h., $L_3 \simeq .15$ μ.h., $L_0 \simeq .1$ μ.h.,

$C_1 = 7$–45 p.f., $C_2 = 200$–250 p.f., $C_3 = 7$–45 p.f.,

$C_0 = 7$–45 p.f., $C_b = .1$ μf, $G_4 = 100\ m\Omega^{-1}$.

Figure 6-1. Experimental Converter Circuit.

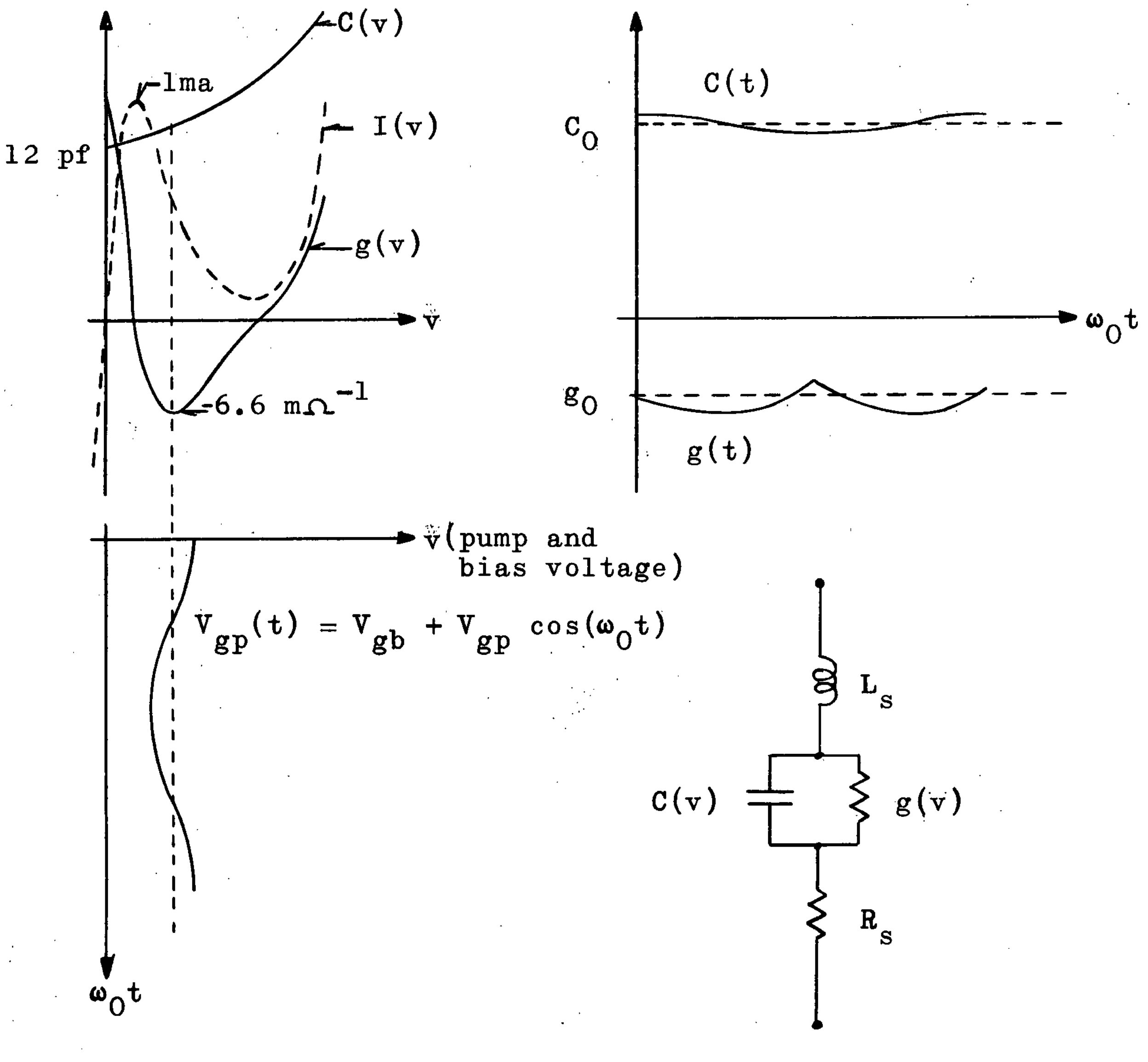

Figure 6-2. Equivalent Circuit and Characteristics of a Pumped IN 2939 Tunnel-Diode.

conductance and capacitance wave forms are approximately:

$g_0 = -4.0 \ m\Omega^{-1}$ $\qquad$ $C_0 = 12.0$ p.f.

$g_1 = -2.0 \ m\Omega^{-1}$ $\qquad$ $C_1 = 2.0$ p.f.

$g_2 = 2.0 \ m\Omega^{-1}$ $\qquad$ $C_2 = 0.5$ p.f.

These values give rise to an α and a β of:

$$\alpha = \frac{\omega_0 C_1}{g_1} = \frac{2\pi \times 100 \times 10^6 \times 2 \times 10^{-12}}{-2.0 \times 10^{-3}} = -0.628$$

$$\beta = \frac{\omega_0 C_0}{g_0} = \frac{2\pi \times 100 \times 10^6 \times 12 \times 10^{-12}}{-4.0 \times 10^{-3}} = -1.9$$

With the parameter values above, the theory predicts that unilateral conversion with gain is possible.

In order that circuit (6-1) be stable at the bias point in the negative conductance region, a d-c stability condition, together with the stability conditions outlined in the theory, (equations 4-13) must be obeyed. The former is satisfied if the conductance (at d-c) across the diode is greater than the absolute value of the diode conductance ($6.6 \ m\Omega^{-1}$). The G_4, G_5 combination provides a suitable value. The latter conditions are satisfied with a margin of safety, if the real part of the admittance across the diode is greater than the absolute value of the diode conductance* at all frequencies below the diode resistive cut-off frequency.(15) In order that the admittance be large, it is essential that wiring inductance be kept to a minimum.

The tuned circuits of the converter are designed to have a high admittance at harmonic frequencies other than their centre frequencies. With such a design the converter is equivalent to the computer analyzed model of Section 4.5. The circuit elements with the exception of $\overline{G}_1$ and $\overline{G}_2$ can therefore be determined from equations AII-2 through AII-6. $\overline{G}_1$ and $\overline{G}_2$ are chosen to give the desired stability and gain. Since lumped elements at V.H.F. frequencies have associated parasitics, the values given by the above equations must be adjusted after the components are mounted in the actual circuit.

In the experimental model, high quality components were used in an effort to minimize parasitic effects. The four inductors, each 3/4" in diameter, were wound with ½ to 3 turns of #14 tinned copper wire. Their Q at 100 mc. was above 50. With such a Q the equivalent coil conductances are small compared to the load conductances. The adjustable capacitors were of the ceramic disc type. The components were placed on a 3/16" shielded brass chassis fitted with standard B.N.C.

---

* If the real part of the admittance is not sufficiently large, self-oscillations will occur. By arranging these oscillations to take place at the pump frequency, it is possible to eliminate the need for an external pump source. Converters of this self-oscillating type(8) were experimented with, but great difficulty was found in controlling the amplitude of the oscillations. Since the adjustments of the converter for directional gain are critical to begin with (Section 6.2), the investigation of self-oscillating converters was not pursued beyond the preliminary stage.

connectors in such a manner that no wiring between the components was required.

6.2 Experimental Techniques and Results

The equipment available for alignment and check-out was all of the 50Ω characteristic impedance type. To provide a match, independent of frequency, between the equipment and the converter, it was necessary to use resistive matching networks at all times. These networks superimposed additional noise on the various signals so that it was not possible to measure the noise figure of the converter.

A sweep-frequency signal generator and a detector were used to align roughly the four tuned circuits.

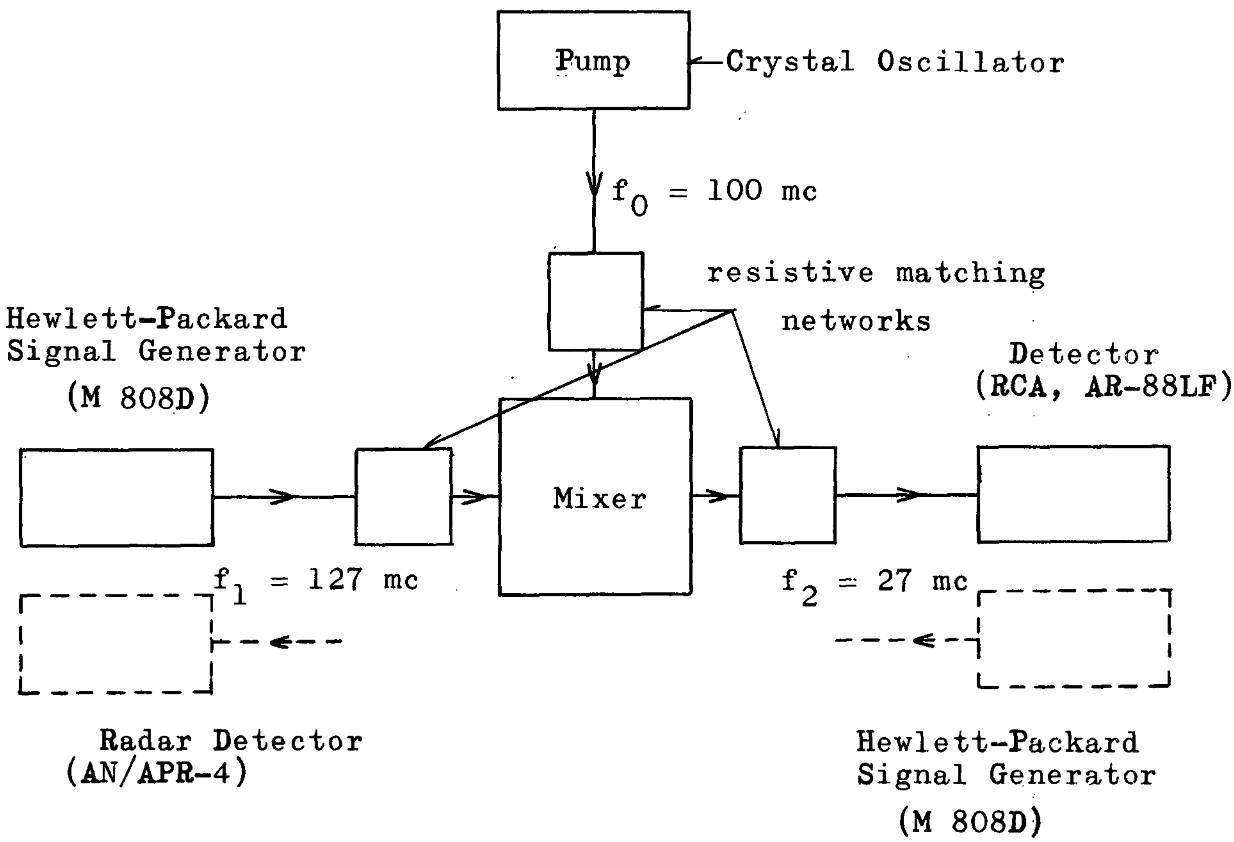

Figure 6-3. Block Diagram of Converter and Measuring Equipment.

Figure 6-3 is a block diagram of the equipment used for fine tuning and measurement of the forward and reverse gains.

The very large forward gain possible in theory was not realized in practice. Considerable effort was expended in a sequence of tuning, load matching and bias point adjustments, in order to obtain 1 db. of forward gain and a reverse gain of about -10 db. at one spot frequency.* An insight into the difficulty is contained in the fact that with slight detuning of any of the tuned circuits in one way, a high forward gain could be realized (25 db.), but for this condition the converter was completely reciprocal as far as measurements could be trusted. It is likely that the detuning substantially alters the effective value of β in equation (4-3) and completely changes the value of Y_3 required for unilateral properties. The response curves of the computer analyzed model (Figures 4-6) indicate that the reverse gain has a very narrow bandwidth: this further explains why the tuning and other adjustments might be difficult.

In short, the experiments show that directional gain can be obtained as predicted for the mathematical model: but that the adjustments to achieve such gain (in the circuit used) are extremely critical.

---

* Precise measurement of the reverse gain was not possible because of the very low signal-to-noise ratio of the signal transmitted to the 127 mc. detector. Measurements were further hampered by the necessity to have the magnitude of all forcing signals small compared to the pump signal (100 mv. p. to p.).

6.3 Suggestions for Further Experimental Study

The experimental study was hindered by high-frequency effects and tuning problems. These difficulties could be overcome in two ways; one, use distributed elements (and work at a still higher frequency); or two, use a tunnel-diode in parallel with a varactor-diode* and work at a lower frequency. Although high frequency experimental work would lead directly to practical applications, work at low frequencies would promote a better understanding of the phenomena involved in unilateral conversion. Furthermore, at low frequencies, it should be possible to obtain wide-band unilateral gain since the optimum terminations (Section 4.2) could be closely approximated.

In addition, an experimental study of a quadrature pumped converter is required to indicate whether such a converter is practical; the study would also provide a realistic comparison of the two methods.

Future experimenting should also be done with circuits suitable for noise figure measurements.

---

* The varactor-diode is required as the nonlinear capacitance of a tunnel-diode is insufficient at low frequencies.

7. CONCLUSIONS

This study has shown that a frequency converter with a passive image termination can provide unilateral down-conversion with gain. For this type of conversion the mixing-element must have both nonlinear capacitance and nonlinear conductance, such as that of a tunnel-diode (Section 4.2). With simple terminations, the unilateral feature is present only over a narrow frequency band (Section 4.5), but with more complex terminations, wide-band unilateral gain can be achieved, (Section 4.4).

The noise mechanism of the converter is extremely complex, but approximate calculations indicate that its noise figure is only slightly worse than that of a bilateral converter (Chapter 5).

Unilateral down-conversion with gain can also be obtained by the quadrature pumping method. Converters using this method require fewer parameters than image terminated converters, but the unilateral property is possible only over a narrow bandwidth.

APPENDIX I

Positive Real Driving-Point Admittance

This appendix deals with the conditions that the image terminating admittance must satisfy in order to be a positive real driving-point admittance.

The image terminating admittance required to give wide-band unilateral gain is, from equation (3-7):

$$Y_3 = -g_0 - j\omega_3 C_0 + \frac{\left(g_2 - j\omega_1 C_2\right)\left(g_1 + j\omega_3 C_1\right)}{g_1 - j\omega_1 C_1}$$

This admittance can be written in terms of the complex frequency variable s by letting $s = j\omega_3$ and also noting that $\omega_1 = 2\omega_0 - \omega_3$.

$$Y_3 = \frac{\begin{aligned} & g_1^2\left(g_2 - g_0\right) + 4\,\omega_0^2 C_1\left(g_1 C_2 - g_0 C_1\right) \\ & + s\;2g_1 C_1\left(g_2 - g_0\right) + g_1^2\left(C_2 - C_0\right) + 4\omega_0^2 C_1^2\left(C_2 - C_0\right) \\ & + s^2\;C_1^2\left(g_2 - g_0\right) + 2g_1 C_1\left(C_2 - C_0\right) \\ & + s^3\;C_1^2\left(C_2 - C_0\right) \\ & + j\;2\omega_0\left(C_1 g_2 - C_2 g_1\right)\left(g_1 + sC_1\right) \end{aligned}}{g_1^2 + 4\omega_0^2 C_1^2 + s\;2g_1 C_1 + s^2\;C_1^2} \qquad \text{...(AI-1)}$$

For this to be a positive real driving-point admittance it is at least necessary that the following conditions be satisfied:[17]

(1) $C_1 g_2 - C_2 g_1 = 0$

(2) $C_2 \geq C_0$

(3) $g_1 C_1 \geq 0$

Condition (2) cannot be satisfied with semiconductor diodes or other known nonlinear capacitance elements.[9] This is sufficient to prove that Y_3 cannot be a positive real driving-point admittance.

APPENDIX II

Terminating Components for a "Practical" Converter

The terminating components are chosen to give the same loading as optimum terminations (Section 4.2) at band-centre.

The equations describing the converter (equations 4-2) can be written in the following simplified form:

$$\begin{bmatrix} \bar{I}_1 \\ 0 \end{bmatrix} = \begin{bmatrix} Y_1 + Y_{11} & Y_{12} \\ Y_{21} & Y_2 + Y_{22} \end{bmatrix} \begin{bmatrix} V_1 \\ V_2 \end{bmatrix} \qquad \ldots(\text{AII-1})$$

Let the normalized angular r.f., i.f. and image band-centre frequencies be denoted by Ω_{10}, Ω_{20} and Ω_{30} respectively. The required loading will be realized if the components of the converter (Figure 4-5) are the following values:

$$L_{if}\, C_{if} = \frac{1}{\Omega^2_{i0}} \qquad i = 1, 2, 3 \qquad \ldots(\text{AII-2})$$

$$\Omega_{10}\, \bar{C}_1 = - I_m(Y_{11})\Big|_{\Omega_1 = \Omega_{10}}$$

$$= -\Omega_{10}\beta g_0 + \frac{g_2\alpha}{1 + \Omega^2_{30}\alpha^2} \qquad \ldots(\text{AII-3})$$

$$\Omega_{20}\overline{C}_2 = -I_m(Y_{22})\Big|_{\Omega_2 = \Omega_{20}}$$

$$= -\Omega_{20}\beta g_0 + \frac{g_1{}^2\alpha}{g_2}\left(\Omega_{10} + \Omega_{20}\right) \qquad \ldots(\text{AII-4})$$

$$\overline{G}_3 + j\Omega_{30}\overline{C}_3 = Y_3\Big|_{\Omega_3 = \Omega_{30}} \qquad \text{from which}$$

$$G_3 = -g_0 + g_2\left(\frac{1 - \Omega_{10}\Omega_{30}\alpha^2}{1 + \Omega_{10}{}^2\alpha^2}\right) \qquad \ldots(\text{AII-5})$$

$$\Omega_{30}\overline{C}_3 = -\Omega_{30}\beta g_0 + \frac{2g_2\alpha}{1 + \Omega_{10}{}^2\alpha^2} \qquad \ldots(\text{AII-6})$$

The inductance and capacitance values given by these equations are normalized with respect to the pump frequency.

Should $\Omega_{i0}\overline{C}_i$ be negative, an inductive termination is required, and $\Omega_{i0}\overline{C}_i$ is replaced by $\dfrac{-1}{\Omega_{i0}\overline{L}_i}$.

These equations determine all but the filter components uniquely. If the L_{if}/C_{if} ratio, which is associated with the bandwidth, is also specified, all components can be determined.

REFERENCES

1. Torrey, H.C. and Whitmer, C.A., Crystal Rectifiers, McGraw-Hill Book Company, Inc., New York and London, (1948).

2. van der Ziel, A., Noise, Prentice-Hall, Inc., Englewood Cliffs, N.J., (1956).

3. Esaki, L., "New Phenomenon in Narrow P-N Junctions", Phys. Rev. Letters, Vol. 109, p. 603, (1958).

4. Edwards, C.F., "Frequency Conversion by Means of a Nonlinear Admittance", Bell Sys. Tech. J., Vol. 35, pp. 1403-16, (November, 1956).

5. Sterzer, F. and Presser, A., "Stable Low-Noise Tunnel-Diode Frequency Converters", RCA Rev., Vol. 23, pp. 3-28, (Mar. 1962).

6. Chang, K.K.N., Heilmeier, G.H. and Prager, H.J., "Low-Noise Tunnel-Diode Down Converters Having Conversion Gain", Proc. IRE, Vol. 48, pp. 854-58, (May, 1960).

7. Cunningham, W.J., Introduction to Nonlinear Analysis, McGraw-Hill Book Company, Inc., New York and London, (1958).

8. Kim, C.S., "Tunnel-Diode Converter Analysis", IRE Trans. PGED, Vol. ED-8, pp. 394-404, (Sept. 1961).

9. Blackwell, L.A. and Kotzebue, K.L., Semiconductor-Diode Parametric Amplifiers, Prentice-Hall, Inc., Englewood Cliffs, N.J., (1961).

10. Pucel, R.A., "Theory of the Esaki Diode Frequency Converter", Solid-State Electronics, Vol. 3, pp. 167-208, (Nov.-Dec. 1961).

11. Englebrecht, R.S., "Parametric Energy Conversion by Nonlinear Admittances", Proc. IRE, Vol. 50, pp. 312-21, (Mar. 1962).

12. Ross, P.W. and Skalnik, J.F., "Parametric Frequency Converters With Arbitrary Pumping Angles", Proc. IRE, Vol. 51, p. 239, (Jan. 1963).

13. Linville, J.G. and Gibbons, J.F., Transistors and Active Circuits, McGraw-Hill Book Company, Inc., New York, Toronto and London, (1961).

14. Manley, J.M., and Rowe, H.E., "Some General Properties of Nonlinear Elements - Part I, General Energy Relations", Proc. IRE., Vol. 44, pp. 904-913, (July 1956).

15. Sommers, H.S., "Tunnel-Diodes as High Frequency Devices", Proc. IRE, Vol. 47, pp. 1201-06, (July 1959).

16. Gärtner, W.W., Transistors: Principles, Design and Applications, D. Van Nostrand Company, Inc., Princeton, N.J., (1960).

17. Guillemin, E.A., Synthesis of Passive Networks, John Wiley and Sons, Inc., New York, (1959).